

# Inductive-resonant mechanism of nonradiative transitions in ions and molecules in condensed phase

V L Ermolaev, E B Sveshnikova, E N Bodunov

## Contents

<b>1. Introduction</b>	<b>261</b>
<b>2. Inductive-resonant theory of nonradiative transitions between electronic levels in the condensed phase</b>	<b>262</b>
2.1 Quantum-mechanical justification of the theory and its applicability limits; 2.2 Position of the inductive-resonant theory among other theories of nonradiative transitions	
<b>3. Comparison between experimental findings and those predicted by the inductive-resonant theory</b>	<b>266</b>
3.1 Ions of trivalent lanthanides in condensed phase; 3.2 Ions of transition metals in solutions, glasses and crystals;	
3.3 Molecules in the condensed phase	
<b>4. Conclusions</b>	<b>280</b>
<b>References</b>	<b>281</b>

**Abstract.** The inductive-resonant mechanism of nonradiative transitions between electronic levels in lanthanide and transition metal ions and complex molecules in the condensed phase is systematically described. A quantum-mechanical justification is presented, and theoretical expectations conforming to the mechanisms and quantitative rate constants of nonradiative transitions are compared with experiment.

*“The most difficult thing is not so much to explain luminescence in the condensed phase as, vice versa, to account for the lack of luminescence in so many molecules”.*  
Vavilov S I *Collected Works*. Vol. 1, p. 222

## 1. Introduction

During the last 70 years, the mechanism of nonradiative transitions between electronic levels of ions and molecules in condensed phase has been a most intriguing problem for those interested in spectroscopy, luminescence, photochemistry, and photobiophysics. Since the early Sixties, it has also attracted the attention of specialists involved in the search, study, and development of laser media (activated glasses, crystals, and solutions). However, despite the great interest of theorists and experimenters in this problem, it remains unclear which approach should be used to estimate nonradiative transition rate constants ( $k_{nr}$ ) in different systems. We discuss below experimental and theoretical evidence of

the possibility to apply the inductive-resonant theory of nonradiative transitions to the mechanism explanation and quantitative calculation of  $k_{nr}$  for a variety of excited centres in the condensed phase.

Nonradiative deactivation of electronic excitation can be achieved through physical or chemical mechanisms. With the physical mechanism, the sole result of deactivation of a molecular or ion electronic excitation is the transition towards a lower-energy electronic state and the transformation of the released energy first to vibrational energy and then to thermal one. Deactivation by the chemical mechanism results in intermediate and final chemical products differing from the starting compound. Typical examples of chemical deactivation mechanisms are photoisomerization and electron transfer.

The present review examines the physical mechanism of nonradiative transitions excepting the well-studied case of deactivation due to the crossing of the potential surfaces of electronic states [1].

The mechanism of nonradiative transitions has been considered in a few monographs [2, 3] and chapters on spectrometry, luminescence, and photochemistry in different books [4–7]. The history of the problem can be traced back to the very early reports on the subject by Engman [2]. Medvedev and Osherov critically reviewed later papers [3]. A wealth of experimental data on nonradiative transitions in ions and molecules, largely in solutions, were collected in Chapter 8 of our monograph [4]. Kaminsky et al. [5], as well as Kaminsky and Antipenko [7] examined different theoretical approaches and experimental findings concerning nonradiative transitions in ions of rare-earth elements inside crystals and glasses activated by them. Taken together, these publications provide the basis for the discussion of our own understanding of the mechanism of nonradiative transitions in the context of the inductive-resonant theory of this phenomenon.

Our approach, first suggested in 1971 [8, 9], is based on the assumption that nonradiative transitions in excited centres like ions of lanthanides and transition metals in the con-

V L Ermolaev, E B Sveshnikova, E N Bodunov Russian Research Centre ‘S I Vavilov State Optical Institute’,  
Birzhevaya liniya 12, 199034 St.-Petersburg, Russia  
Tel. (7-812) 213 90 33 ad 22 91  
Fax (7-812) 218 21 33  
E-mail: ermol@soi.spb.su

Received 22 June 1995, revised 27 November 1995  
*Uspekhi Fizicheskikh Nauk* 166 (3) 279–302 (1996)  
Translated by Yu V Morozov, edited by A Radzig

densed phase (solutions, glasses, crystals) together with simple and organic molecules in solutions are induced by resonant interactions between electronic or vibronic oscillators, which correspond to radiative transitions to lower-energy electronic (vibronic) levels, and isoenergetic vibrational oscillators of molecular groups surrounding the excited centre. The quantum-mechanical justification of this approach will be given below. Now, it is worthwhile to emphasise that interactions of this type between the said oscillators always occur whenever molecular groups around the excited centre exhibit purely vibrational absorption spectrum overlapping the emission spectrum of the centre. The problem is whether this phenomenon is largely responsible for nonradiative transitions in the condensed phase or its contribution to the process that determines the rate of nonradiative transitions is relatively small. The present paper contains experimental evidence that the postulated mechanism of nonradiative transitions is equally relevant for a broad range of excited centres in the condensed phase.

In the context of our approach, the mechanism of nonradiative transitions is reminiscent of nonradiative transfer of electronic excitation energy suggested by Forster [10]. The two approaches are different in that the energy acceptor in the former case is supposed to be purely vibrational transition rather than the vibronic transition in the Forster theory. Similar to the model underlying the Forster theory, energy transfer to oscillations is assumed to be rapidly followed by the rejection of excessive vibrational energy both in the excited centre and in the molecular groups around it. Vibrational relaxation rates in the condensed phase reported in the literature [11] indicate that in most cases of nonradiative transitions for the excited centres in the condensed phase discussed below, this condition is explicitly fulfilled. Figure 1 presents energy-level diagram pertaining to the above mechanism.

Many theoretical studies have been published since the late Sixties concerned with the irreversible nature of non-radiative transitions, the relationship between electronic and vibrational relaxation in the final electronic state, and the preparation of the excited state as a result of the interaction between the optical centre or a molecule and exciting electromagnetic radiation. Readers are referred for more details on these issues to the aforementioned monographs [2, 3]. The present review is limited to nonradiative transitions in optical centres in the condensed phase. On the one hand, these systems are more complicated than individual molecules, but on the other hand they are simpler because there is the possibility of the unambiguous solution to the problem of irreversibility and compliance with the case of ‘statistical limit’ (after terminology of J Jortner) [12].

## 2. Inductive-resonant theory of nonradiative transitions between electronic levels in the condensed phase

### 2.1 Quantum-mechanical justification of the theory and its applicability limits

According to the previously developed formal theory of nonradiative transitions [2, 3], excitation results in the non-stationary excited state. Its nature depends on the properties of the system (polyatomic molecule, impurity centre in a crystal, glass or solution) and the spectral and temporal characteristics of the excitation process. Given the relatively

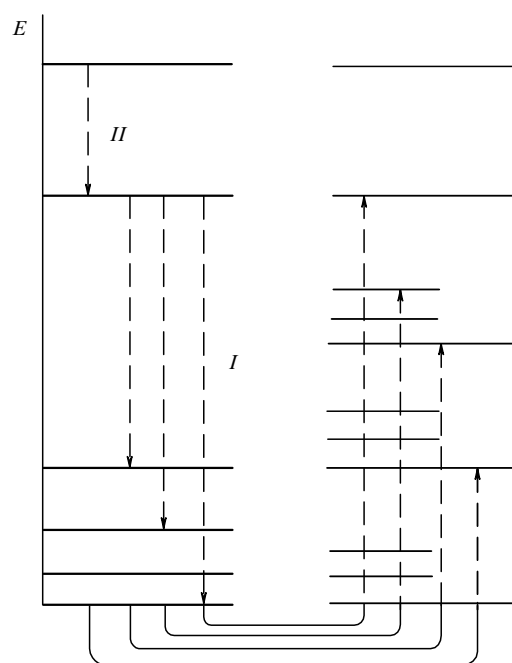


**Figure 1.** Schematic diagram of energy levels illustrating the inductive-resonant theory of nonradiative transitions for the case of weak vibronic coupling ( $\text{Ln}^{3+}$  ions): *I*—multiphonon nonradiative transition, *II*—one-phonon nonradiative transition. Bold lines on the left-hand side denote electronic levels, thin lines on the right-hand side are levels of donor-acceptor oscillations. Vertical dotted lines depict the process of donor-acceptor energy transfer responsible for nonradiative transitions between electronic levels and excitation of resonant transitions between vibrational levels.

small duration of the exciting pulse and the sufficiently high density of the final states, radiationless decay of the initial non-stationary state is exponential, and its rate ( $k_{\text{nr}}$ ) can be calculated in the first order of the time-dependent perturbation theory.

It is worthwhile to emphasise that the formal theory should not be considered a recipe for estimating  $k_{\text{nr}}$  in a given system. However, it has important physical implications which suggest the necessity of choosing adiabatic Hamiltonian as the zero Hamiltonian  $H_0$ , the eigenfunction of which stands for the initial state. Then, the perturbation  $V$  which induces nonradiative transitions is the difference between the total Hamiltonian of the system  $H$  and the zero Hamiltonian  $H_0$  ( $V = H - H_0$ ), i.e. the non-adiabaticity operator. Therefore, the theory that facilitates computation of  $k_{\text{nr}}$  in specific systems is based on the following assumptions.

1. The adiabatic approximation is correct. Wave function of the system  $\Psi_{mb}(\mathbf{r}, \mathbf{Q})$  can be written as the product of electronic wave function  $\varphi_m(\mathbf{r}, \mathbf{Q})$  and vibrational function  $\chi_b(\mathbf{Q})$ :

$$H_0 \Psi_{mb}(\mathbf{r}, \mathbf{Q}) = E_{mb} \Psi_{mb}(\mathbf{r}, \mathbf{Q}),$$

$$\Psi_{mb}(\mathbf{r}, \mathbf{Q}) = \varphi_m(\mathbf{r}, \mathbf{Q}) \chi_b(\mathbf{Q}). \quad (1)$$

Here,  $m = 0, 1$  for the ground and excited states, respectively,  $b$  is the set of vibrational quantum numbers,  $\mathbf{r}(r_1, r_2, \dots)$  — electronic coordinates,  $\mathbf{Q} = \{Q_1, Q_2, \dots\}$  — nuclear coordinates, and  $E_{mb}$  is the energy of the electronic-vibrational state.

2. Adiabatic wave functions are not eigenfunctions of the total Hamiltonian  $H$  of the system. Therefore, the non-adiabaticity operator  $V$  is responsible for nonradiative transitions between different adiabatic electronic states. This operator has only nondiagonal (in electronic quantum numbers) nonzero matrix elements which take the form

$$V_{0a,1b} = - \sum_i \frac{\hbar^2}{M_i} \int d\mathbf{Q} \chi_{0a}(\mathbf{Q}) \left\langle \varphi_0(\mathbf{r}, \mathbf{Q}) \left| \frac{\partial}{\partial Q_i} \right| \varphi_1(\mathbf{r}, \mathbf{Q}) \right\rangle \frac{\partial}{\partial Q_i} \chi_{1b}(\mathbf{Q}) + \frac{1}{2} \sum_i \frac{\hbar^2}{M_i} \int d\mathbf{Q} \chi_{0a}(\mathbf{Q}) \left\langle \varphi_0(\mathbf{r}, \mathbf{Q}) \left| \frac{\partial^2}{\partial Q_i^2} \right| \varphi_1(\mathbf{r}, \mathbf{Q}) \right\rangle \chi_{1b}(\mathbf{Q}), \quad (2)$$

where  $M_i$  is the mass of  $i$ -th nucleus. Normally, the unessential term containing the second derivatives of electronic wave functions with respect to nuclear coordinates are neglected in this expression. After this, formula (2) can be transformed to

$$\left\langle \varphi_0(\mathbf{r}, \mathbf{Q}) \left| \frac{\partial}{\partial Q_i} \right| \varphi_1(\mathbf{r}, \mathbf{Q}) \right\rangle = \frac{\langle \varphi_0(\mathbf{r}, \mathbf{Q}) | \partial U / \partial Q_i | \varphi_1(\mathbf{r}, \mathbf{Q}) \rangle}{E_0(\mathbf{Q}) - E_1(\mathbf{Q})}. \quad (3)$$

Here,  $U(\mathbf{r}, \mathbf{Q})$  is the Coulomb energy of electron-nucleus interaction,  $E_0(\mathbf{r}, \mathbf{Q})$  and  $E_1(\mathbf{r}, \mathbf{Q})$  are adiabatic potentials in the ground and excited states, respectively.

Rough estimates of (3) at the equilibrium positions of nuclear coordinates (the so-called Condon approximation:  $Q_i = 0$ ) lead to

$$\left\langle \varphi_0(\mathbf{r}, \mathbf{Q}) \left| \frac{\partial}{\partial Q_i} \right| \varphi_1(\mathbf{r}, \mathbf{Q}) \right\rangle = \frac{\langle \varphi_0(\mathbf{r}, \mathbf{Q}) | \partial U / \partial Q_i | \varphi_1(\mathbf{r}, \mathbf{Q}) \rangle \Big|_{Q_i=0}}{E_0 - E_1}, \quad (4)$$

where  $E_0$  and  $E_1$  are the adiabatic potentials for the equilibrium nuclear configuration.

3. Interferential effects between different channels of nonradiative transitions are neglected. This allows the total rate  $k_{nr}$  of transitions between states 1 and 0 to be written as the sum of partial transition probabilities:

$$k_{nr} = \frac{2\pi}{h} \sum_{a,b} |V_{0a,1b}|^2 p(1b) \delta(E_{0a} - E_{1b}). \quad (5)$$

Here,  $p(1b)$  is the population of an initial electronic-vibrational state described by quantum numbers 1 and  $b$ .

4. It is supposed that the initial (excited) electronic state is characterised by the equilibrium distribution over vibrational sublevels during the entire period of nonradiative transition. This is possible if the vibrational relaxation rate significantly exceeds that of the nonradiative transition  $1 \rightarrow 0$ . Then

$$p(1b) = \exp \frac{E_{1b}}{kT} \left( \sum_b \exp \frac{E_{1b}}{kT} \right)^{-1}. \quad (6)$$

5. The vibrational wave function is represented as the product of wave functions of normal oscillators

$$\chi_{1b}(\mathbf{Q}) = \prod_i \Phi_{1i}(Q_i, m_i), \quad (7)$$

where  $m_i$  is the index of the vibrational sublevel of the corresponding normal oscillator  $i$ ,  $b = \{m_i\}$ .

When estimating  $k_{nr}$ , it is usually assumed that normal coordinates and frequencies of normal oscillations are the same in the ground and electronically excited states. In the course of electronic transition, only the equilibrium position of the nuclei is altered, i.e. there occurs a shift in the equilibrium position of normal oscillators. Normal oscillations are considered to be harmonic disregarding anharmonism. Our derivation of the expression for  $k_{nr}$  in the systems of interest is also based on the generally accepted scheme (points 1–5) [5, 13, 14]. However, we make one more assumption to specify the media under study which is widely used in practice.

Let us assume that oscillations with different properties in the systems under study can be categorized into two groups [14]. Let us further denote them by labels  $k$  and  $j$ , respectively. The shape of the adiabatic potential of type 1 oscillations ( $k$ ) shows but weak dependence on whether the system is in the ground or excited state. Therefore, the wave functions in states 0 and 1 may be supposed to coincide for these oscillations:

$$\Phi_{1k}(Q_k, m_k) = \Phi_{0k}(Q_k, m_k). \quad (8)$$

Energies of vibrational sublevels counted from the bottom of the respective adiabatic potential also coincide:

$$E_{1k}(m_k) = E_{0k}(m_k). \quad (9)$$

These oscillations arise in vibrational absorption spectra of the system. Anharmonism and frequencies of these oscillations are equally high. This means that oscillations of the first type are largely involved in the formation of the vibrational absorption spectrum of the system in both the fundamental and overtone frequency regions. Such oscillations are inapparent in electronic-vibrational spectra because the Franck–Condon integrals are almost zero:

$$\langle \Phi_{1k}(Q_k, m_k) | \Phi_{0k}(Q_k, n_k) \rangle \approx 0, \quad m_k \neq n_k. \quad (10)$$

Type 1 oscillations include, for instance, valent oscillations of O–H, O–D, C–H, C–D, N–H, N–D groups and also oscillations of Si–O, Ge–O, P–O, Zr–F, Li–F, and other groups in glasses and crystals.

Conversely, the adiabatic potential of type 2 oscillations ( $j$ ) is subject to marked changes during transition of a system (molecule, impurity centre) from the ground state to the excited one. This may be apparent as altered frequencies and equilibrium positions of normal oscillators. These oscillations form an electronic-vibrational spectrum of the system because the Franck–Condon integrals are significantly different from zero:

$$\langle \Phi_{1j}(Q_j, m_j) | \Phi_{0j}(Q_j, n_j) \rangle \neq 0, \quad m_j \neq n_j. \quad (11)$$

These oscillations are often totally symmetric and inapparent in the vibrational absorption spectra of the system. Their frequencies, anharmonism, and interaction with type 1 oscillations are insignificant, and they are not responsible for vibrational absorption of the system in the radiative transition region. In case of aromatic molecules, they are totally symmetric C–C oscillations whereas for complexes and solvates of transition metals and lanthanides — oscillations of the ion and the nearest neighbour atoms.

The use of the non-adiabaticity operator as a perturbation source which induces nonradiative transitions and categorisation of oscillations into two groups allowed us to show in Ref. [14] that, as in the theory of nonradiative energy transfer [4, 15], the nonradiative transition rate  $k_{nr}$  can be expressed through the overlap integral over the normalised electronic-vibrational emission spectrum  $f(E)$  of the system and the cross-section  $\sigma(E)$  of vibrational absorption in the same system:

$$k_{nr} \sim \overline{\left\langle \varphi_0 \left| \frac{\partial U}{\partial Q_k} \right| \varphi_1 \right\rangle}^2 \int f(E) \sigma(E) E^{-(s+1)} dE, \quad (12)$$

where the bar denotes averaging over type 1 oscillations ( $k$ ).

This became possible because according to our assumptions the spectral shape  $f(E)$  is virtually determined by oscillations of the second type ( $j$ ) through the Franck–Condon integrals

$$f(E) \sim E^s \left| \prod_j \langle \Phi_{0j}(m_j) | \Phi_{1j}(n_j) \rangle \right|^2 \quad (13)$$

( $s = 3$  with dipole radiation and  $s = 5$  with quadrupole radiation) while  $\sigma(E)$  depends on type 1 oscillations through integrals

$$\sigma(E) \sim E \left| \langle \Phi_{0k}(m_k) | Q_k | \Phi_{0k}(n_k) \rangle \right|^2. \quad (14)$$

When calculating the electronic matrix element  $\langle \varphi_0 | \partial U / \partial Q_k | \varphi_1 \rangle$ , one may confine oneself to the dipole approximation, that is

$$\overline{\left\langle \varphi_0 \left| \frac{\partial U}{\partial Q_k} \right| \varphi_1 \right\rangle}^2 \sim \frac{|\langle \varphi_0 | e\mathbf{r} | \varphi_1 \rangle|^2}{R^6} \chi^2$$

( $\chi$  is the orientation factor and  $\overline{\chi^2} \sim 2/3$ ,  $R$  is the effective distance between the vibronic and type 1 vibrational oscillators). Therefore, it follows from (12)–(14) that at  $s = 3$ ,

$$k_{nr} = \frac{9h^4 c^4 k_r \chi^2}{8\pi n^4 R^6} \int f(E) \sigma(E) E^{-4} dE. \quad (15)$$

Here,  $k_r$  is the radiative transition rate, and  $n$  is the refractive index of the medium.

Turning to the wave numbers  $\nu$  instead of energy  $E$ , the molar decimal extinction coefficient  $\varepsilon_{vib}(\nu)$  instead of  $\sigma(E)$ , and the luminescence spectrum normalised to unit area  $I_1^n(\nu)$  instead of  $f(E)$ , one finds the following expression from (15):

$$k_{nr} = \frac{9000 \ln 10 \chi^2 k_r}{128\pi^5 n^4 N_A R^6} \int I_1^n(\nu) \varepsilon_{vib}(\nu) \nu^{-4} d\nu. \quad (16)$$

Formula (16) essentially coincides with the Forster formula which describes transfer of electronic excitation energy through the dipole-dipole mechanism [16, 17] and differs from it only in that the energy acceptor is the electronic oscillator rather than the vibrational one. The integral in formulas (12), (15) and (16) is referred to as the overlap integral over luminescence and vibrational absorption spectra of the surrounding donor-acceptor groups and is denoted hereinafter as  $\int_{ov}$ .

The presence of the effective distance in (15) and (16) is justified by the following considerations. It is known from vibrational spectroscopy [18] that high-frequency oscillations of the CH, NH, OH type are characteristic local oscillations. Also, oscillations of non-bridging atomic groups like BO, PO in glasses are largely local [19]. For this reason, when examining deactivation of lanthanide ( $\text{Ln}^{3+}$ ) ions and ions of transition metals in solutions, glasses, and molecules, one can speak about distance  $R$  between the electronic oscillator localised on the ion, and the vibrational oscillator located on a group of atoms responsible for absorption.

Expansion of the electrostatic electron-nucleus interaction potential in multipoles is possible if the condition  $R \gg r$ , where  $r$  is the linear multipole size, holds. This condition is surely satisfied for the electronic-vibrational interaction between metal ions and the medium since  $r$  for the multipole moment of intraconfiguration transition in the ion is smaller than the size of  $f$ - and  $d$ -shells, i.e. less than 0.05–0.06 nm. The size of the vibrational absorbing dipole is comparable with that of the amplitude of atomic oscillations near their equilibrium positions (i.e.  $\sim 0.01$  nm) while  $R$  normally lies in the range from 0.2 to 1 nm. Thus, the above conditions being fulfilled, the nonradiative deactivation of the excited state of the system (molecule, complex, solvate, etc.) may be regarded as nonradiative energy transfer of electronic excitation from the vibronic oscillator to the resonant vibrational oscillator, and the rate of this process can be estimated using formulas (12), (16). In so doing, one part of electronic energy is spent to induce type 2 oscillations ( $j$ ) while the other is utilised to excite oscillations of the first type ( $k$ ), which are not appreciably affected by electronic excitations. The effect of either part depends on the anharmonic contribution to the type 1 oscillations and on changes in equilibrium positions and frequencies of type 2 oscillators during electronic transition. This is automatically taken into account when computing the overlap integral  $\int_{ov}$  over spectra in (12), (16).

It is worthwhile to note that (1) condition  $r \ll R$  is not always fulfilled in certain systems (e.g. crystals like  $\text{LaF}_3$ ,  $\text{Y}_2\text{O}_3$ ) which makes it impossible to expand the electronic matrix element in powers of parameter  $r/R$ ; nevertheless, there is direct proportionality between  $k_{nr}$  and the overlap integral, in conformity with formulas (14)–(16); (2) condition  $r \ll R$  is met, but the contribution to the electronic matrix element (15) is due, in agreement with the selection rules, to higher terms of its expansion in  $r/R$  (e.g. the quadrupole term); in this case, proportionality between  $k_{nr}$  and the overlap integral is likewise preserved although  $R$ -dependence alters.

Deviation from the proportionality between  $k_{nr}$  and the overlap integral over spectra may be expected to occur only when quadrupole (and higher order) transitions between type 1 vibrational states need to be taken into consideration, as suggested in Ref. [20]. However, it will be shown in the experimental section below that such cases have never been observed.

The following is also noteworthy. Although formula (12) was derived as based on the separation of normal oscillations, this is actually unessential for electronic-vibrational energy transfer. It is sufficient to separate type 1 and 2 oscillations. Within these two groups, oscillations may interact, which would result in the appearance of combined frequencies in the respective spectra, and these interactions will be taken into account in the estimation of  $k_{nr}$ .

## 2.2 Position of the inductive-resonant theory among other theories of nonradiative transitions

It has been mentioned above that since early studies reported in [21, 22], the non-adiabaticity operator (1) has been used as perturbation to induce nonradiative transitions, first in the form of (4) in which the energy denominator does not depend on the nuclear coordinates. This approximation is termed the Condon approximation. Kovarsky and co-workers [23] have demonstrated that this approximation leads to the underestimation of the transition probability. They suggested the so-called non-Condon approximation in which the non-adiabaticity operator has the form of (3) and where an energy denominator depends on the nuclear coordinates. The  $k_{nr}$  values computed in the non-Condon approximation are  $N^2$  times higher than those obtained with the Condon approximation ( $N$  is the number of phonons produced during nonradiative transition). This finding was later confirmed in Ref. [24].

The static coupling model focussed to calculate  $k_{nr}$  has been independently developed in [25, 26]. This model uses the nondiagonal component of the electron-phonon interaction as a transition-triggering perturbation (in fact only its linear part in atomic displacements from the equilibrium position). This part is taken into account in the first order of the perturbation theory. The diagonal-in-electronic-states part is included in the electronic Hamiltonian, namely, it is considered exactly. According to calculations,  $k_{nr}$  values in the static coupling model are also  $N^2$  times higher than those obtained in the Condon approximation.

Finally, it has been shown in [27] that the non-Condon approximation in which both items of (2) must be taken into account in the non-adiabaticity operator, is totally equivalent to the static coupling model. Kovarsky et al. [28] appear to share this opinion. It should be noted that such equivalence has also been found in one particular case by Bodunov and Sveshnikova [29].

Thus, let  $U$  be the operator of electron-phonon interaction in the system under examination. Expansion of this interaction energy in powers of small atomic displacements from the equilibrium position (in a series in normal coordinates) yields

$$U = \sum_i \frac{\partial U}{\partial Q_i} Q_i + \sum_i \frac{\partial^2 U}{\partial Q_i \partial Q_s} Q_i Q_s + \dots \quad (17)$$

The diagonal-in-electronic-states part of this interaction leads to a shift in equilibrium positions of oscillators during electronic transition (first item in (17)) and a change in vibrational frequencies and the Dushinsky effect (second item in (17)).

Given a certain symmetry of the equilibrium position, oscillations may be categorized as totally symmetric or partially symmetric, depending on whether the symmetry of the system is lowered or not during these oscillations.

It follows from the theory of groups that there is no shift in the equilibrium position for partially symmetric oscillations. As far as frequency changes and the Dushinsky effect are concerned, they can always occur in both totally and partially symmetric oscillations.

It has already been noted that the nondiagonal component of the electron-phonon interaction (more specifically, only its first (linear in  $Q_i$ ) item in (17)) is used as perturbation inducing nonradiative transitions. If the ground and excited states have different parity, the nondiagonal matrix element of this item is other than zero only for partially symmetric oscillations. It is interaction with these oscillations (termed

donor oscillations) that is taken by the majority of authors as the perturbation to calculate  $k_{nr}$ . Since these oscillations are considered to be harmonic (the interaction is linear in the normal coordinates), a nonradiative transition can give rise to only one phonon of the partially symmetric oscillation. The remaining (major) part of the electronic energy is spent on exciting totally symmetric oscillations (which are therefore referred to as acceptor oscillations).

To summarise, the traditional approach also distinguishes between two types of oscillations:

(1) donor oscillations, i.e. harmonic partially symmetric oscillations lacking in a shift of the equilibrium position during electronic transition;

(2) acceptor oscillations, i.e. harmonic totally symmetric oscillations undergoing a shift of the equilibrium position during electronic transition.

In later studies [5, 7], calculations of  $k_{nr}$  for rare-earths in crystals were carried out using low-frequency oscillations from the phonon spectrum of the crystal as donor oscillations and both totally symmetric (undergoing a shift of the equilibrium position) and partially symmetric (undergoing frequency changes during electronic transition) oscillations as acceptor ones. It has been shown that such an approach yields  $k_{nr}$  values in accord with those obtained experimentally only at  $E_1 - E_0 \leq 2000 \text{ cm}^{-1}$  [5]. Therefore, the mechanism of nonradiative transitions for  $E_1 - E_0 > 2000 \text{ cm}^{-1}$  was considered in which the  $N$ -phonon transition is generated by the  $N$ -th term of the expansion of electron-phonon interaction energy (17) in nuclear displacements from the equilibrium position [30–33]. Many authors emphasise that this approach yields good results at  $N < 6$  but fails to ensure accuracy at  $N > 6$  [5, 30, 31, 33].

It is inferred from the comparison of the traditional and inductive-resonant approaches that the inductive-resonant theory also distinguishes between two types of oscillations:

(a) acceptor oscillations, i.e. totally symmetric oscillations undergoing a shift of the equilibrium position during electronic transition and partially symmetric oscillations with variable frequency; they are apparent in the electronic vibrational spectra of emission or absorption;

(b) donor-acceptor oscillations, i.e. anharmonic oscillations, the interaction wherewith generates nonradiative transitions; they experience neither a shift of the equilibrium position nor frequency changes during electronic transition; due to their anharmonicity, nonradiative transitions can give rise to several phonons pertaining to these oscillations rather than to the sole phonon as in the traditional approach.

It is clear that when anharmonism is disregarded, donor-acceptor oscillations simply turn to donor ones, and the two approaches coincide. By taking into consideration anharmonicity of oscillations, the inductive-resonant theory allows (through integrals over overlapping spectra) for additional channels of relaxation with excitation of two or more phonons of the donor-acceptor oscillations. Therefore, the inductive-resonant theory provides a more general approach.

Let us now compare the accuracy of  $k_{nr}$  calculations using the two approaches. There are some difficulties inherent in the traditional approach:

1. One needs to know the symmetry of the molecule or the nearest neighbours of the ion in the medium (atomic coordinates and interatomic distances). Such information is necessary to construct the Hamiltonian of the system and the potential of electron-phonon interaction. These data may not be readily available.

2. One needs to know wave functions of the system being studied and the structure of electronic levels. This problem is often solved by semi-empirical methods.

3. One needs to know the phonon spectrum of the system (molecule, crystal), a major source of information being the shape of luminescence and absorption spectra (their phonon wings). However, due to the transition selection rules a different set of oscillations may contribute to these spectra as opposed to the process of nonradiative transitions. Hence, a detailed analysis of this process is necessary.

4. When computing  $k_{nr}$  for certain systems (e.g. ions of rare-earth metals in crystals), heat release constants (shifts of equilibrium positions, changes of vibrational frequencies) cannot be determined from experimental data. They have to be determined theoretically. The accuracy of such calculations depends on the accuracy with which the Hamiltonian of the system and electron-phonon interaction potential is defined. Since heat release constants determine the exponential portion of  $k_{nr}$  dependence on temperature and electric gap  $E_1 - E_0$  (through the Franck – Condon integrals (12)), a small inaccuracy in their magnitudes may result in grossly erroneous  $k_{nr}$  values.

Evidently, the accuracy of  $k_{nr}$  calculations in the traditional approach is rather low due to a very high sensitivity of the nonradiative transition rate to parameters of the given system.

Also, the following observation made in [34] should be borne in mind. The adiabatic theory does not provide an exact result. It can only give the correct exponent which defines the dependence of  $k_{nr}$  on temperature and energy gap, and the correct order of the pre-exponential factor in the expression for  $k_{nr}$ . This is so because when determining the pre-exponent in the calculation of  $k_{nr}$ , it is inappropriate to be confined to the first order approximation in nondiagonal elements of the electron-phonon interaction, since further orders can also make comparable contribution.

Let us now turn to the inductive-resonant theory. This approach assumes that the overlap integral over spectra which determines the exponential dependence of  $k_{nr}$  on temperature and energy gap can be found from the observed spectra. This allows for the possibility of calculating it rather exactly. The nondiagonal-in-electronic-states part of the electron-phonon interaction energy depends on  $k_r$ ,  $R$ , and  $\varkappa$ . The  $k_r$  value is either derived from the experimental data or calculated ones using the Judd – Ofelt theory [35] (for  $\text{Ln}^{3+}$  ions). As a rule, data on the geometric structure of the system under examination are available; therefore parameters  $R$  and  $\varkappa$  are also known. However, it is the accuracy of their determination that is believed to limit exact calculation of  $k_{nr}$  with formula (16) and, hence, the accuracy of the inductive-resonant theory in the dipole-dipole approximation.

To conclude, it has been shown that the inductive-resonant approach naturally ensues from the general theory of nonradiative transitions, and it is more general than traditional approaches due to its taking into account the anharmonism of oscillations. The accuracy of calculation of nonradiative transition rate constants with the inductive-resonant approach is sufficiently high because it is a semi-empirical method based on experimental data.

The inductive-resonant theory predicts the following (see formula (16)):

(1) the exponential dependence of  $k_{nr}$  on energy gap  $\Delta E_{el}$ , in agreement with the exponential-like decrease of  $I_1^n(\nu)$  and

$\varepsilon_{vib}(\nu)$  spectra with increasing  $\nu$ ; (2) the deviation from the exponential  $\Delta E_{el}$  dependence of  $k_{nr}$  in the structured regions of  $I_1^n(\nu)$  and  $\varepsilon_{vib}(\nu)$  spectra; (3) proportionality between  $k_{nr}$  and  $k_r$  which can be broken down only in the case of strict limitation on the symmetry of electric dipole transitions; (4)  $k_{nr}$  dependence on anharmonicity of oscillations through  $\varepsilon_{vib}(\nu)$ .

The existence of the electronic-vibrational energy transfer in the condensed phase has been unequivocally demonstrated in Ref. [36]. The authors observed emission in a CsBr crystal from four vibrational levels of  $\text{CN}^-$  anion excited by means of electronic-vibrational energy transfer from the  $F$ -centre located in the immediate vicinity of  $\text{CN}^-$  groups.

The objective of experimental studies is to clarify whether the inductive-resonant mechanism (specifically, formula (16)) is the major one contributing to nonradiative transition rates in a variety of condensed phase objects. This issue is approached in Section 3.

### 3. Comparison between experimental findings and those predicted by the inductive-resonant theory

#### 3.1 Ions of trivalent lanthanides in condensed phase

**3.1.1 Solutions.** In 1965, Kropp and Windsor [37] reported a marked effect of solvent deuteration on the luminescence quenching rate in aqueous  $\text{Eu}^{3+}$  ( $^5\text{D}_0$ ) and  $\text{Tb}^{3+}$  ( $^5\text{D}_4$ ) solutions. The luminescence quenching time ( $\tau_1$ ) for these ions in deuterated water was estimated to be 32 and 8.4 times longer, respectively, than  $\tau_1$  in natural water [38]. This finding is consistent with the ‘physical’ mechanism of nonradiative transitions under these conditions. It has also been shown [38–40] that  $k_{nr}$  in lanthanide ( $\text{Ln}^{3+}$ ) ions exhibits linear dependence on the molar fraction of  $\text{H}_2\text{O}$  in the  $\text{H}_2\text{O}$ – $\text{D}_2\text{O}$  mixture. This suggests that electronic energy dissipation occurs with excitation in the donor-acceptor group of only one highly excited vibrational state rather than several oscillations in the molecular groups surrounding the ion.

The authors of this paper first suggested the inductive-resonant theory of nonradiative transitions in 1971 with special reference to  $\text{Ln}^{3+}$  ions in solutions [8, 9]. From the standpoint of the requirements of the inductive-resonant theory for energy transfer,  $\text{Ln}^{3+}$  ions make very simple objects because electronic and vibrational motions in them are hardly related and can be regarded as independent, electronic transition is localised inside the 0.05 nm  $4f$ -shell, and the distance to the nearest high-frequency vibrational level (e.g. asymmetric valent vibration of the ion-linked O–H-group in water) is 0.26–0.22 nm (the former value is for the beginning of the lanthanide group and the latter, for its second half).

In previous studies [8, 9, 13, 41], we investigated the possibility of predicting the effect of solvent deuteration on  $k_{nr}$  by calculating the overlap integral ( $\int_{ov}$ ) over luminescence spectra and vibrational absorption spectra of the environment and obtained the  $\int_{ov}^H / \int_{ov}^D$  ratio for  $\text{Ln}^{3+}$  ions in H- and D-containing solvents. Table 1 shows the results of these calculations and compares them with the ratios of the observed nonradiative transition rate constants in the same systems ( $k_{nr}^H/k_{nr}^D$ ). It follows from the comparison that theoretical and experimental data are in good agreement for both multiphonon ( $\text{Tb}^{3+}$ ,  $\text{Eu}^{3+}$ ,  $\text{Dy}^{3+}$ , etc.) and one-phonon

**Table 1.** The ratio between the overlap integrals over  $\text{Ln}^{3+}$  luminescence spectrum and vibrational absorption spectra for protonated and deuterated solvents as compared with the ratio of experimentally obtained nonradiative transition rate constants in the same solvents (from [8, 9, 13, 41])

$\text{Ln}^{3+}$	Transition	Luminescence spectrum region, $\text{cm}^{-1}$	Solvent	$\frac{\int_{\text{D}}^{\text{H}}}{\int_{\text{D}}^{\text{D}}}$	$\frac{k_{\text{nr}}^{\text{H}}}{k_{\text{nr}}^{\text{D}}}$
$\text{Eu}^{3+}$	${}^5D_0 - \sum {}^7F_i$	17250–12150	$\text{H}_2\text{O}; \text{D}_2\text{O}$	38	48
$\text{Yb}^{3+}$	${}^2F_{5/2} - {}^2F_{7/2}$	10300	$\text{H}_2\text{O}; \text{D}_2\text{O}$	29	25
$\text{Dy}^{3+}$	${}^4F_{9/2} - \sum {}^6F_i; {}^6H_j$	20800–7400	$\text{H}_2\text{O}; \text{D}_2\text{O}$	18	20
$\text{Nd}^{3+}$	${}^4F_{3/2} - \sum {}^4I_i$	11400–5000	$\text{H}_2\text{O}; \text{D}_2\text{O}$	9	5
$\text{Er}^{3+}$	${}^4I_{11/2} - {}^4I_{13/2}$	3600	$\text{H}_2\text{O}; \text{D}_2\text{O}$	80	100
$\text{Er}^{3+}$	${}^4I_{11/2} - {}^4I_{13/2}$	3600	$(\text{CH}_3)_2\text{SO}$ $(\text{CD}_3)_2\text{SO}$	3	4.5
$\text{Pr}^{3+}$	${}^3P_0 - {}^1D_2$	3500	$(\text{CH}_3)_2\text{SO}$ $(\text{CD}_3)_2\text{SO}$	5	3
$\text{Eu}^{3+}$	${}^5D_1 - {}^5D_0$	1750	$(\text{CH}_3)_2\text{SO}$ $(\text{CD}_3)_2\text{SO}$	—	1

( $\text{Er}^{3+}$ ) transitions which suggests the possibility to use the inductive-resonant theory for the explanation of the effect of deuteration on  $k_{\text{nr}}$  values of such transitions in  $\text{Ln}^{3+}$  ions.

The overlap integral in formula (16) fairly well accounts for the inverse exponential dependence of the nonradiative transition rate constant for  $\text{Ln}^{3+}$  ions in solutions on the minimal energy gap between levels undergoing deactivation and the nearest lower-lying level. It equally well explains a deviation from this relationship. Figure 2 shows dependence of  $\log k_{\text{nr}}$  (from resonance levels for some  $\text{Ln}^{3+}$  ions in methanol- $d_1$  at 293 K) on the minimal energy gap  $\Delta E_{\text{el}}^{\text{min}}$  between the emitting level and its nearest low-lying neighbour. It appears from Fig. 2 that the points for  $\text{Sm}^{3+}$ ,  $\text{Dy}^{3+}$ ,  $\text{Eu}^{3+}$ , and  $\text{Tb}^{3+}$  fall on the straight line, whereas  $k_{\text{nr}}$  value for  $\text{Yb}^{3+}$  lies two orders of magnitude above. In the context of the inductive-resonant theory, this deviation looks quite natural for the following reason. The spectrum of  $\text{Yb}^{3+}$  ions in

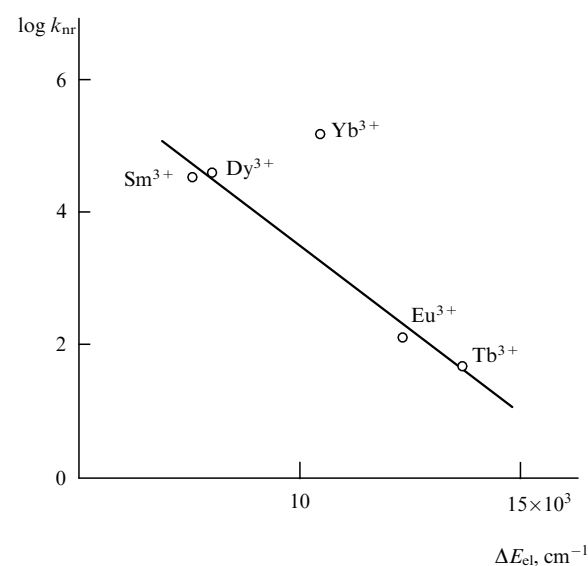


**Figure 2.** Logarithmic dependence of rate constant for nonradiative transitions from resonance levels of  $\text{Ln}^{3+}$  ions ( $\text{Tb}^{3+} - {}^5D_4$ ,  $\text{Eu}^{3+} - {}^5D_0$ ,  $\text{Dy}^{3+} - {}^4F_{9/2}$ ,  $\text{Sm}^{3+} - {}^4G_{5/2}$ ,  $\text{Yb}^{3+} - {}^2F_{5/2}$  in methanol- $d_1$  at 293 K) on the energy difference between the emitting and the nearest lower-lying levels [41].

solution at room temperature consists of one band corresponding to the transition between two levels separated by interval  $\Delta E_{\text{el}}^{\text{min}}$ . At the same time, long-wavelength luminescence bands for the other four ions corresponding to the minimal energy gap, constitute but a small part ( $\sim 0.01$ ) of the total luminescence area. Taking into consideration that formula (16) contains luminescence spectrum normalised to unit area, it is easy to account for the difference between the overlap integrals and the resulting marked deviation of  $k_{\text{nr}}$  point for  $\text{Yb}^{3+}$ .

When the overlapping between the  $\text{Ln}^{3+}$  luminescence spectrum and the vibrational absorption spectrum of donor-acceptor groups, which determines the overlap integral in formula (16), occurs in the overtone absorption region, anharmonism (both mechanical and electro-optical) of donor-acceptor oscillations starts playing an important role. Convincing experimental evidence on the role of anharmonicity in electronic excitation energy dissipation has been obtained in a study [42] designed to evaluate the contribution of two molecular groups,  $\text{C}\equiv\text{N}$  and  $\text{C}-\text{D}$ , with similar vibrational frequencies (2254 and 2257  $\text{cm}^{-1}$ , respectively) but significantly different in terms of anharmonicity, to nonradiative transitions from the  ${}^4F_{9/2}$  level of  $\text{Dy}^{3+}$  ion dissolved in dehydrated deuterated acetonitrile. This study has shown that the nonradiative transition from  ${}^4F_{9/2}$  is induced by highly anharmonic oscillations of the  $\text{CD}_3$  rather than  $\text{C}\equiv\text{N}$ -group even though the latter group in the solution is directly coordinated with  $\text{Dy}^{3+}$  ion while  $\text{CD}_3$ -group is located 0.5 nm apart. This can be accounted for by the fact that the vibrational absorption spectrum in the region where it overlaps the  $\text{Dy}^{3+}$  luminescence spectrum is almost completely determined by the absorption of the  $\text{CD}_3$ -group.

The inductive-resonant theory, like other theories of nonradiative transitions, predicts that if electronic energy dissipation occurs on oscillations with  $h\nu > kT$ , there is no temperature dependence of  $k_{\text{nr}}$  because  $\int_{\text{ov}}$  does not change. Therefore, temperature dependence of  $k_{\text{nr}}$  in solutions of  $\text{Ln}^{3+}$  ions indicates that a change of  $T$  brings about a change in the immediate environment of the ions.

For the majority of transitions in  $\text{Ln}^{3+}$  ions, radiation takes the form of that for a forced electric dipole [43], and the conditions for the expansion of electronic-vibrational interaction energy in multi-fields are satisfied. Therefore, it can be expected that the first term of the series corresponding to the electric dipole-dipole interaction will make the greatest contribution to the  $k_{\text{nr}}$  quantity. In this case,  $k_{\text{nr}}$  can be calculated using a formula which resembles the Forster formula for the dipole-dipole energy transfer between complex organic molecules, the only difference being that the absorption spectrum is represented by the vibrational absorption spectrum of the molecular groups surrounding  $\text{Ln}^{3+}$  ions instead of the electronic-vibrational spectrum of the acceptor. Calculations are facilitated by the use of formula (18), an analog of formula (16) which takes into account the possibility of interaction between the electronic oscillator and several vibrational oscillators located at different distances from the ion as well as the number of these vibrational groups:

$$k_{\text{nr}} = 8.8 \times 10^{-25} n^{-4} \kappa^2 k_{\text{r}} \left( \sum_i N_i R_i^{-6} \int I_i^n(\nu) \varepsilon_{\text{vib}}^i(\nu) \nu^{-4} d\nu + \sum_j N_j R_j^{-6} \int I_j^n(\nu) \varepsilon_{\text{vib}}^j(\nu) \nu^{-4} d\nu \right), \quad (18)$$

where  $k_r$  is the rate constant of downward radiative transition from a given level (in  $\text{s}^{-1}$ );  $I_1^n(\nu)$  is the dimensionless intensity distribution in the emission spectrum (luminescence spectrum normalised to unit area on the wave number scale);  $\alpha_{\text{vib}}^i(\nu)$  is the molar decimal coefficient of vibrational absorption (in  $\text{cm}^2 \text{mmol}^{-1}$ ) of the  $i$ -th donor-acceptor groups located at distance  $R_i$  from the excitation centre;  $\kappa^2$  is the orientation factor normally assumed to be averaged and equal to  $2/3$ ;  $n$  is refractive index of the medium;  $\nu$  is the wave number (in  $\text{cm}^{-1}$ );  $R = |\mathbf{R}|$  is the distance (in cm) between the electronic excitation centre and vibrational oscillators interacting with this centre; finally,  $N_i$  and  $N_j$  are the molecular group numbers.

The feasibility of using formula (18) for calculating  $k_{\text{nr}}$  in  $\text{Ln}^{3+}$  ions can be tested in the following ways: (a) by estimating the dependence of an experimentally observed nonradiative transition rate constant in ions on the distance to donor-acceptor molecular groups, and (b) by comparing theoretical  $k_{\text{nr}}^{\text{calc}}$  values obtained according to formula (18) and experimental  $k_{\text{nr}}^{\text{exp}}$  values.

It appears impracticable to experimentally realise a model system in which an individual donor-acceptor molecular group is located at a variable distance from the excited ion. It is however possible, using  $\text{Ln}^{3+}$  solutions, to realise systems showing no donor-acceptor oscillations around the excited ion in the sphere of variable radius  $a$ . If the molecular groups outside the sphere with radius  $a$  exhibit almost identical vibrational spectra overlapping with luminescence spectra and the number of donor-acceptor groups in a unit volume of the solvent is roughly the same, it will be possible to use the formula derived by Galanin and Frank [44] for the electric dipole emitting in the continuous absorbing medium:

$$k_{\text{nr}} = k_r (16\pi^4 n^4 a^3)^{-1} \int I_1^n(\nu) \alpha_{\text{vib}}(\nu) \nu^{-4} d\nu, \quad (19)$$

where  $a$  is the radius of the sphere around the ion (in cm) containing no molecular groups responsible for donor-acceptor oscillations, and  $\alpha_{\text{vib}}(\nu)$  is the linear absorption coefficient (in  $\text{cm}^{-1}$ ) of donor-acceptor oscillations outside the sphere of radius  $a$ , the medium around the latter being regarded as continuous. See formula (18) for other notations.

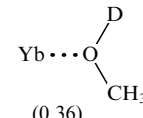
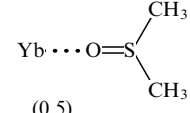
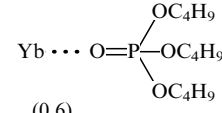
According to the inductive-resonant theory, there must be a proportional dependence of  $k_{\text{nr}}$  on the product  $k_r a^3$  for different transitions in  $\text{Ln}^{3+}$  ions in the identical environment provided all luminescence transitions have electric dipole nature.

We have experimentally realised a case very similar to the above model by placing  $\text{Yb}^{3+}$  and  $\text{Dy}^{3+}$  ions into such solvents as  $\text{CH}_3\text{OD}$ ,  $(\text{CH}_3)_2\text{SO}$ , and  $(\text{C}_4\text{H}_9\text{O})_3\text{PO}$  [13, 45, 46]. It is known from chemistry of coordination compounds [47, 48] that  $\text{Ln}^{3+}$  ions in these solvents are bound to solvent molecules via the oxygen atom. Donor-acceptor oscillations in this case are valent oscillations of C–H-groups with the highest frequency ( $\sim 3000 \text{cm}^{-1}$ ) and anharmonicity. Oscillations of other groups in the same molecules occur with much lower frequencies and anharmonicity and do not substantially contribute to the deactivation of these ions, for which  $\Delta E_{\text{el}}^{\text{min}} > 7800 \text{cm}^{-1}$ . This observation is confirmed by a sharp decrease in  $k_{\text{nr}}^{\text{exp}}$  for  $\text{Yb}^{3+}$  and  $\text{Dy}^{3+}$  ions in completely deuterated analogs of the solvents in question.

Proceeding from formula (19) on the assumption that  $\alpha_{\text{vib}}(\nu)$ ,  $I_1^n(\nu)$  and  $k_r$  are constant, one obtains  $k_{\text{nr}}^{\text{exp}}$  quantity inversely proportional to  $a^3$ . Table 2 illustrates experimental

values of  $k_{\text{nr}}^{\text{exp}}$  and product  $k_{\text{nr}}^{\text{exp}} a^3$  (in conventional units). The table shows that product  $k_{\text{nr}}^{\text{exp}} a^3$  remains constant within the limits of experimental accuracy ( $\sim 25\text{--}30\%$ ), which confirms both the electric dipole-dipole nature of the interaction leading to nonradiative transitions and the possibility of calculating them with formulas (18), (19).

**Table 2.**  $k_{\text{nr}}$  dependence on the distance between  $\text{Yb}^{3+}$  and donor-acceptor vibrational oscillators [46]

Fragments with complex structure (Yb–CH <sub>n</sub> distance, nm)	Yb <sup>3+</sup> ( <sup>5</sup> F <sub>5/2</sub> )		
	$k_{\text{nr}} \times 10^4, \text{s}^{-1}$	$k_{\text{nr}} a^3, \text{conv. units}$	$k_{\text{nr}} a^5, \text{conv. units}$
 (0.36)	22	1.0	1.0
 (0.5)	5.5	0.67	1.29
 (0.6)	4.5	0.95	2.6

We have so far examined cases where oscillations of molecules directly bound to the  $\text{Ln}^{3+}$  ion made a major contribution to the deactivation of its excited state. However, according to the inductive-resonant theory, the presence or the absence of chemical bonding between an ion and surrounding molecules should not affect  $k_{\text{nr}}$  unless frequencies, anharmonicity, and the distance between the ion and the molecular groups undergo alteration. Moreover, rather slow degradation of the strength of interaction between electric dipoles ( $R^{-6}$ ) implies the possibility to observe  $k_{\text{nr}}$  dependence on the molecular groups located sufficiently far from the deactivated ion with which they are not bound by chemical bonds. This case may be illustrated by the effect exerted on  $\tau_1$  by complexes of  $\text{Ln}^{3+}$  ions with ordinary and deuterated tributyl phosphates of the solvent located more than 1.0 nm from the ion. Table 3 shows the quenching times of  $\text{Sm}^{3+}$  and  $\text{Nd}^{3+}$  complexes with ordinary (TBP- $h_{27}$ ) and completely deuterated (TBP- $d_{27}$ ) tributyl phosphates in toluene- $h_8$  and  $\text{CCl}_4$ . It appears from the comparison of  $\tau_1$  and  $k_{\text{nr}}$  in the solvent ( $\text{CCl}_4$ ) containing no molecular groups capable of promoting nonradiative transitions in  $\text{Sm}^{3+}$  and  $\text{Nd}^{3+}$  and in toluene- $h_8$  (whose molecules exhibit high-frequency donor-acceptor oscillations of C–H-groups) that a solvent located far from the ion (on a molecular size scale)

**Table 3.** Effect of donor-acceptor oscillations in molecular groups located 10 Å from the ions (at 293 K) on  $k_{\text{nr}}$  values in  $\text{Ln}^{3+}$  ions (from [45])

Complex	$\tau_1, \mu\text{s}$	$k_{\text{nr}}, \text{s}^{-1}$		Contribution of the solvent to $k_{\text{nr}}, \text{s}^{-1}$
		toluene- $h_8$	$\text{CCl}_4$	
$\text{Sm}(\text{NO}_3)_3(\text{TBP-}d_{27})_3$	350	1100	2500	600
$\text{Sm}(\text{NO}_3)_3(\text{TBP-}h_{27})_3$	—	130	—	7700
$\text{Nd}(\text{NO}_3)_3(\text{TBP-}h_{27})_3$	2.1	3.0	480000	330000



makes an important contribution to the nonradiative transition rate constant.

We have previously calculated  $k_{nr}^{calc}$  using formulas (18), (19) in [8, 9, 13, 49]. The calculation of interactions with the help of formula (18) taking into account each molecule surrounding the ion is impracticable, the more so since their location in the solution is largely obscure. Therefore, the first sphere surrounding the  $Ln^{3+}$  ion and involving molecules of usually known positions and number, was taken into consideration in calculations with formula (18) while other molecules of the solvent were taken into account by formula (19). Table 4 contains  $k_{nr}^{calc}$  values thus obtained in different solvents and compares them with experimental  $k_{nr}^{exp}$  values.

The theoretical and experimental data appear to be in rather good agreement, bearing in mind that no adjustable parameters were used in the calculation. Possible errors in determining  $k_{nr}^{calc}$  with formulas (18) and (19) will be discussed below.

Another weighty argument in favour of our interpretation on the mechanism of nonradiative transitions is the possibility to explain the unusually low probability of nonradiative transitions between levels  ${}^5D_1 - {}^5D_0$  in  $Eu^{3+}$  [50] and  ${}^3P_1 - {}^3P_0$  in  $Pr^{3+}$  [51] during which radiation of the magnetic dipole type is emitted. An example of transitions for which  $k_{nr}^{exp}$  can be accurately measured is provided by the  ${}^5D_1 - {}^5D_0$  transition in  $Eu^{3+}$ . The energy gap for this transition is about  $1750\text{ cm}^{-1}$ , which means that  $k_{nr}$  must be in excess of  $10^{10}\text{ s}^{-1}$  if the nonradiative transition mechanism in this case was identical with that of other transitions in  $Ln^{3+}$  ions (see Table 4).

Actually,  $k_{nr} = \tau^{-1} ({}^5D_1)$  in different media is  $10^5 - 10^6\text{ s}^{-1}$  [50]. It is known from the theory [17, 44] that the rate constant for the nonradiative energy transition through the mechanism of interaction between magnetic and electric dipoles is many orders of magnitude lower than for the interaction between two electric dipoles and can be described by the formula

$$k_{nr}(md) = k_r(4\pi^2 an)^{-1} \int I_1^n(v) \alpha_{vib}(v) v^{-2} dv, \quad (20)$$

where  $k_r$  is the radiative constant of magnetic-dipole transition (in  $\text{cm}^{-1}$ ). All other notations in formula (20) are the same as in (18) and (19).

The required value for the  ${}^5D_1 - {}^5D_0$  transition of  $Eu^{3+}$  ion in an acetone solution was found to be  $k_{nr}^{calc} = 1.1 \times 10^4\text{ s}^{-1}$  when calculated with the formula for the magnetic dipole decay in a continuous absorption medium (acetone) [50, 52].

The computation was carried out using an acetone vibrational absorption spectrum in which the valent vibrational frequency for the C = O-group is similar to the energy gap of  ${}^5D_1 - {}^5D_0$  transition, and  $k_r = \tau_1^{-1}$  related to  ${}^5D_1$ -level of  $Eu^{3+}$  in halide crystals, which may lead to overestimation of the actual  $k_r$  value. Thus obtained  $k_{nr}$  turned out to be one and a half orders of magnitude lower than the value found in the experiment. The distance between  $Eu^{3+}$  ion and atomic oxygen in the C = O group was used as the radius of the sphere containing molecules with donor-acceptor type of oscillations. Also, it has been shown in Refs [53, 54] that limiting probabilities for one-phonon nonradiative transitions in  $Ln^{3+}$  ions vary from  $10^{11}$  to  $10^{12}\text{ s}^{-1}$  regardless of the base and decrease to  $10^{10}\text{ s}^{-1}$  in the case of resonance disturbance in radiative electronic and vibrational transitions.

Disregarding the magnetic-dipole nature of  ${}^5D_1 - {}^5D_0$ , calculations with formula (19) for the electric dipole-dipole interaction yield  $k_{nr}^{calc} \geq 10^{11}\text{ s}^{-1}$ , which is six orders of magnitude higher than the experimentally found value. It was judiciously assumed in [50] that the observed  $k_{nr}$  value is due to a small admixture of the electric dipole transition into the magnetic-dipole one and its interaction with oscillations of the environment molecules. This hypothesis is supported by the fact that the  $k_{nr}$  value for the  ${}^5D_1 - {}^5D_0$  transition increases with symmetry decreasing in the environment of the  $Eu^{3+}$  ion, which facilitates removal of the forbiddenness upon electric dipole transitions [50, 52]. Therefore, once the radiative transition between levels is actually of a magnetic dipole nature, then the rate constant of nonradiative transitions between these levels must be anomalously low, as predicted by the inductive-resonant theory and actually observed in the experiment [55, 56].

Also, using the inductive-resonant theory to calculate  $k_{nr}$  for  $Ln^{3+}$  ions in solutions is known to be in error. To begin with, rapid ligand exchange between ions of lanthanides and molecules of the solvent in liquid solutions results in the averaged picture. Hence,  $\tau_1$  and  $k_{nr}$  must be dependent of a rapidly changing conformation of the ion's environment. Quenching of luminescence remains exponential as long as the ligand exchange time is less than  $\tau_1$ . Non-exponential quenching occurs when the exchange time equals or exceeds  $\tau_1$ , and several types of complexes with different  $\tau_1$  co-exist in the solution. The exchange time of water molecules for  $Ln^{3+}$  ions at room temperature is on the order of  $10^{-7}\text{ s}$  [57].

**Table 4.** Comparison of nonradiative transition rate constants ( $k_{nr}^{calc}$ ,  $\tau_1^{calc}$ ) for  $Ln^{3+}$  ions in solutions calculated in the framework of the inductive-resonant theory and their values obtained experimentally under the same conditions. The calculation was performed within the approximation of electric dipole interactions ( $T = 293\text{ K}$ ) (from [8, 9, 13, 49])

$Ln^{3+}$	Transition $\Delta E_{el}, \text{cm}^{-1}$	Solvent	$k_r, \text{s}^{-1}$	$\tau_1^{calc}, \text{s}$	$k_{nr}^{calc}, \text{s}^{-1}$	$\tau_1^{exp}, \text{s}$	$k_{nr}^{exp}, \text{s}^{-1}$
$Er^{3+}$	${}^4S_{3/2} - {}^4F_{9/2}$	$(\text{CH}_3)_2\text{SO}$	13	$5.6 \times 10^{-9}$	$1.8 \times 10^8$	$1.3 \times 10^{-8}$	$8 \times 10^8$
	3100	$(\text{CD}_3)_2\text{SO}$	13	$4.5 \times 10^{-8}$	$2.2 \times 10^7$	$9 \times 10^{-8}$	$1.1 \times 10^7$
$Er^{3+}$	${}^4I_{11/2} - {}^4I_{13/2}$	$\text{H}_2\text{O}$	13	$4 \times 10^{-11}$	$2.5 \times 10^{10}$	$1.2 \times 10^{-10}$	$8.3 \times 10^9$
	3590	$\text{D}_2\text{O}$	13	$3.2 \times 10^{-9}$	$3.1 \times 10^8$	$1.2 \times 10^{-8}$	$8.3 \times 10^7$
$Er^{3+}$	${}^4I_{11/2} - {}^4I_{13/2}$	$\text{CD}_3\text{OH}$	16	$6 \times 10^{-10}$	$1.8 \times 10^9$	$7.7 \times 10^{-10}$	$1.3 \times 10^9$
	3710	$\text{CD}_3\text{OD}$	16	$1.1 \times 10^{-8}$	$9.1 \times 10^7$	$3.3 \times 10^{-8}$	$3 \times 10^7$
$Pr^{3+}$	${}^1D_2 - {}^1G_4$	$\text{CD}_3\text{OH}$	870	$9 \times 10^{-6}$	$1.1 \times 10^5$	$1.5 \times 10^{-6}$	$6.7 \times 10^5$
	7000						
$Nd^{3+}$	${}^4F_{3/2} - \sum {}^4I_i$	$\text{D}_2\text{O}$	2500	$1.2 \times 10^{-6}$	$8.3 \times 10^5$	$4 \times 10^{-8}$	$2.5 \times 10^7$
$Sm^{3+}$	${}^4G_{5/2} - \sum {}^6F_i \sum {}^6H_j$	$\text{H}_2\text{O}$	370	$6.7 \times 10^{-6}$	$1.5 \times 10^5$	$3 \times 10^{-6}$	$3.3 \times 10^5$
	18000-8000						
$Yb^{3+}$	${}^2F_{5/2} - {}^2F_{7/2}$	$\text{H}_2\text{O}$	1500	$2 \times 10^{-7}$	$5 \times 10^6$	$1.7 \times 10^{-7}$	$5.9 \times 10^6$
	10300	$\text{D}_2\text{O}$	1500	$6 \times 10^{-6}$	$1.7 \times 10^5$	$4.2 \times 10^{-6}$	$2.4 \times 10^5$
$Dy^{3+}$	${}^4F_{9/2} - \sum {}^6F_i \sum {}^6H_j$	$\text{CH}_3\text{OH}$	300	$2.4 \times 10^{-5}$	$4.2 \times 10^4$	$9 \times 10^{-6}$	$1.1 \times 10^5$
	20800-7000	$\text{CD}_3\text{OD}$	300	$3.6 \times 10^{-4}$	$2.8 \times 10^3$	$1.5 \times 10^{-4}$	$6.6 \times 10^3$

Another source of errors in  $k_{nr}$  calculation is a poor knowledge of relative positions of ligands and solvent molecules about the ion. Also, the error may be due to the fact that in most cases the spectrum of a pure solvent is used as the vibrational absorption spectrum instead of the spectrum of molecules directly coordinated with the ion. Absorption spectra of the latter molecules, especially those of OH-groups in water or alcohols and NH-groups of amines in which the oxygen (nitrogen) atom is directly bound to the ion, differ in the vibrational frequency and anharmonicity from analogous spectra for groups of molecules located outside the first coordination sphere of the ion [58]. Nevertheless, comparison of  $k_{nr}$  calculated with the inductive-resonant theory and obtained experimentally in water and hydrated crystals indicates that, even for water, changes in vibrational frequencies and anharmonicity in the course of water-ion coordination are not crucial for  $k_{nr}$  calculation.

In most cases, mutual arrangement of dipole moments of electronic transitions in an ion and vibrational absorption in its environment are not taken into account because formula (18) uses the averaged quantity  $\kappa^2 = 2/3$ . Large error in  $k_{nr}$  calculation is also due to the  $k_r$  quantity in formulas (18), (19), especially when its experimental determination is difficult and one has to use the value calculated by the Judd–Ofelt method.

**3.1.2 Glasses and crystals.** The mechanism of nonradiative transitions in  $\text{Ln}^{3+}$  ions in glasses and crystals has been investigated in many articles [5, 53] in which various modes of nonradiative transitions, from shear ([5], p. 125) to non-linear [59] ([5], p. 150), have been discussed. Great interest in the mechanism of nonradiative transitions in these systems is largely due to an important, frequently critical, role of these processes in the effective operation of lasers on the base of glasses and crystals activated by different lanthanide ions.

Let us try to explain experimental facts pertaining to  $\text{Ln}^{3+}$ -activated glasses and crystals in the context of the inductive-resonant theory. It is known from crystal chemistry that in  $\text{Ln}^{3+}$ -containing crystal hydrates of the  $\text{GdCl}_3 \cdot 6\text{H}_2\text{O}$ ,  $\text{GdCl}_3 \cdot 6\text{D}_2\text{O}$  type, the immediate milieu of the  $\text{Ln}^{3+}$  ion is formed by water and resembles the nearest environment of the ion in aqueous solutions. In an earlier study [60], we investigated luminescence of  $\text{Dy}^{3+}$  ions added to  $\text{GdCl}_3 \cdot 6\text{H}_2\text{O}$  and  $\text{GdCl}_3 \cdot 6\text{D}_2\text{O}$  crystals as a 1% impurity along with vibrational absorption spectra of  $\text{GdCl}_3 \cdot 6\text{H}_2\text{O}$  crystals (using a specially grown 2.5 cm long crystal).

The knowledge of the structure of  $\text{Ln}^{3+}$  crystallohydrates, the spectra of water vibrational absorption in these structures, and  $\text{Dy}^{3+}$ -luminescence spectra in crystals provided the basis for a rather accurate calculation of  $k_{nr}$  for  $\text{Dy}^{3+}$ . Table 5 compares theoretical and observed  $k_{nr}$  values for downward transitions from the  ${}^4F_{9/2}$  level of  $\text{Dy}^{3+}$ . It can be seen that these values differ by not more than 25%. Table 5 also shows

**Table 5.** Comparison of experimental and theoretical  $k_{nr}$  values pertaining to the  ${}^4F_{9/2}$  level of  $\text{Dy}^{3+}$  in  $\text{GdCl}_3 \cdot 6\text{H}_2\text{O}$ ,  $\text{GdCl}_3 \cdot 6\text{D}_2\text{O}$  crystals and aqueous solution (at 293 K) (from [60])

Matrix	Calculated values		Experimental values	
	$k_{nr}, \text{s}^{-1}$	$\tau_1, \mu\text{s}$	$k_{nr}, \text{s}^{-1}$	$\tau_1, \mu\text{s}$
$\text{GdCl}_3 \cdot 6\text{H}_2\text{O}$	$2 \times 10^5$	5	$2.5 \times 10^5$	4
$\text{GdCl}_3 \cdot 6\text{D}_2\text{O}$	—	—	$1.5 \times 10^4$	67
$\text{H}_2\text{O}$	$1.2 \times 10^5$	8.3	$3.3 \times 10^5$	3
$\text{D}_2\text{O}$	$6.5 \times 10^3$	210	$1.6 \times 10^4$	60

$\tau_1$  quantity for  $\text{Dy}^{3+}$  in water at room temperature which is not much less than that in the crystal. Therefore,  $\tau_1$  which is almost completely (99%) determined by the nonradiative transition rate, merely undergoes minor changes in passing from solution to crystal since the nearest environment of  $\text{Dy}^{3+}$  in water and crystal differs only in the degree of water molecule fixation near the ion and is essentially similar in terms of distance between the ion and water molecules and the number of these molecules in the inner sphere of the ion.

May and Richardson [61] have proved that water molecules in the second sphere of  $\text{Eu}^{3+}$  ion in the  $\text{Na}_3[\text{Eu}(\text{C}_4\text{H}_4\text{O}_5)_3] \cdot 2\text{NaClO}_4 \cdot 6\text{H}_2\text{O}$  crystal make an important contribution to deactivation of the  ${}^5D_0$ -level in  $\text{Eu}^{3+}$ . It has been experimentally found that the contribution of six water molecules (spaced 0.505 nm from  $\text{Eu}^{3+}$ ) to the  $k_{nr}$  value of the  ${}^5D_0$ -level amounts to  $264 \text{ s}^{-1}$ . Moreover, the same authors [61] have demonstrated that this value essentially agrees with contributions to  $k_{nr}$  by water molecules from the first coordination sphere in crystals  $\text{Eu}(\text{OH})_9(\text{C}_2\text{H}_5\text{SO}_4)_3$  and  $\text{EuCl}_3 \cdot 6\text{H}_2\text{O}$  on the assumption of  $R^{-6}$ -dependence of the contribution from one  $\text{H}_2\text{O}$  molecule to  $k_{nr}$  for the  ${}^5D_0$ -level of  $\text{Eu}^{3+}$ , in compliance with formula (18) in which  $R$  is the distance between the ion and water molecule. Blasse and Dirksen [62] have also shown that nonradiative transitions in  $\text{Eu}^{3+}$ -activated  $(\text{NH}_4)_3\text{YCl}_6$  crystals are initiated by  $\text{NH}_4^+$ -groups located in the second coordination sphere of  $\text{Eu}^{3+}$ .

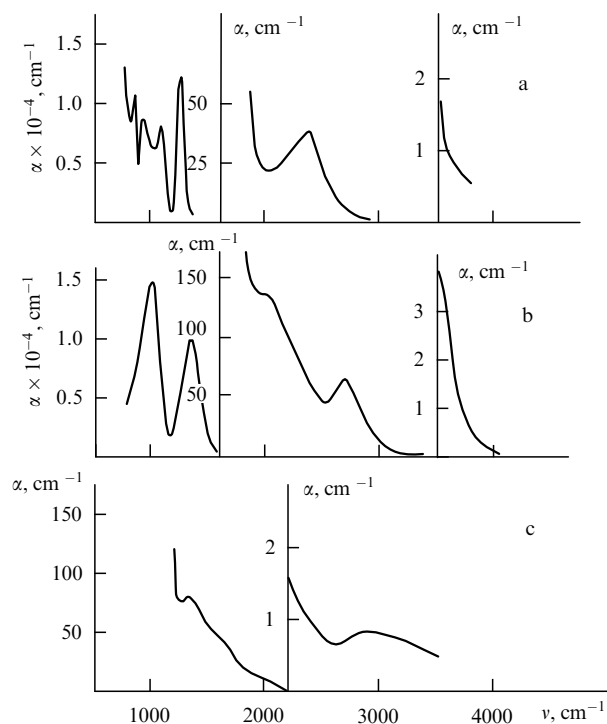
Applicability of the inductive-resonant theory of nonradiative transitions was confirmed for  $\text{Er}^{3+}$ ,  $\text{Tm}^{3+}$ , and  $\text{Nd}^{3+}$ -activated germanate, phosphate, and borate glasses, in which nonradiative transitions with  $\Delta E_{\text{el}}^{\text{min}} < 5000 \text{ cm}^{-1}$  were investigated. In this system, valent oscillations of B–O ( $\nu_{\text{vib}} = 1335 \text{ cm}^{-1}$ ), P–O ( $\nu_{\text{vib}} = 1250 \text{ cm}^{-1}$ ) or Ge–O ( $\nu_{\text{vib}} = 820 \text{ cm}^{-1}$ ) groups were found to be responsible for donor-acceptor oscillations. Calculations were made using formula (19) where the radius of the sphere  $a$ , i.e. the distance between  $\text{Ln}^{3+}$  ion and oxygen atom, was taken equal to 0.25 nm for all  $\text{Ln}^{3+}$  ions.

Table 6 presents experimental and theoretical values of  $k_{nr}$  for certain transitions in ions  $\text{Pr}^{3+}$ ,  $\text{Nd}^{3+}$ ,  $\text{Ho}^{3+}$ ,  $\text{Er}^{3+}$ ,  $\text{Tm}^{3+}$ . Evidently, the calculated values are in good agreement with the experimental ones. Calculations were carried out using measured  $\alpha(\nu)$  values for phosphate, borate, and germanate glasses (Fig. 3) [63]. Figure 3 shows that the first overtones of valent P–O, B–O, Ge–O oscillations is two orders of magnitude less intensive than the fundamental tone, while the second overtone is further about two orders of magnitude less intensive than the first one. This is how absorption of valent oscillations in glasses differs from that corresponding to the absorption of valent X–H(D) oscillations (X = O, C, N), where the first overtone differs in intensity from the fundamental vibrational frequency by one order of magnitude. The difference between each previous overtone and the next one is roughly the same. Therefore, anharmonism of valent oscillations of boron, phosphorous, and germanium-containing groups is much smaller than that of hydrogen or deuterium-containing groups. This effects a steeper exponential dependence of  $k_{nr}$  on the energy gap (expressed as the number of donor-acceptor vibrational quanta) compared with that for the H and D-containing solvents, in which donor-acceptor oscillations are in fact valent oscillations of X–H(D) groups with strong anharmonicity.

It is clear from Table 6 that the experimental and theoretical values do not largely differ by more than one order of magnitude.

**Table 6.** Comparison of experimental  $k_{nr}$  values and calculated from the inductive-resonant theory for  $\text{Ln}^{3+}$  ions in glasses. Data for crystallised glasses (at 293 K) are given in parentheses (from [63, 64])

$\text{Ln}^{3+}$	Transition	$\Delta E_{el}, \text{cm}^{-1}$	Glass	$h\nu_{vib}, \text{cm}^{-1}$	$k_r^{ed}, \text{s}^{-1}$	$k_{nr}^{exp}, \text{s}^{-1}$	$k_{nr}^{calc}, \text{s}^{-1}$
$\text{Er}^{3+}$	$^4I_{13/2} - ^4I_{15/2}$	4800	Borate	1335	—	$1.6 \times 10^4$	$5.6 \times 10^3$
$\text{Er}^{3+}$	$^4I_{11/2} - ^4I_{13/2}$	3870	Phosphate	1250	18	$9 \times 10^5$ ( $2 \times 10^5$ )	$4.1 \times 10^5$
$\text{Pr}^{3+}$	$^3P_0 - ^1D_2$	3850	Phosphate	1250	10	$3.5 \times 10^6$	$2 \times 10^5$
$\text{Tm}^{3+}$	$^3F_4 - ^3H_5$	3750	Germanate	820	—	5	—
$\text{Er}^{3+}$	$^4S_{3/2} - ^4F_{9/2}$	3030	Phosphate	1250	8.7	$1.5 \times 10^6$ ( $1.3 \times 10^6$ )	$2 \times 10^6$
$\text{Ho}^{3+}$	$^5S_2, ^5F_4 - ^5F_5$	2960	Phosphate	1250	9	$10^7$	$4.5 \times 10^6$
$\text{Ho}^{3+}$	$^5F_5 - ^5I_4$	2500	Phosphate	1250	0.1	$5 \times 10^6$	$10^6$

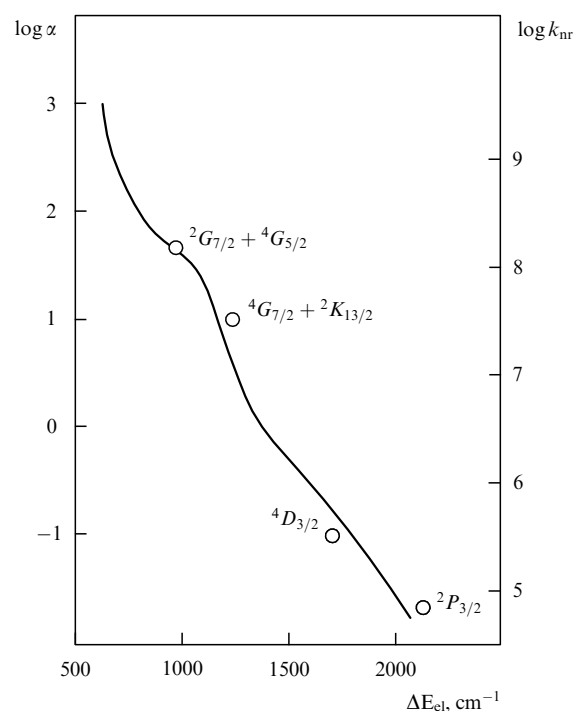
**Figure 3.** Vibrational absorption spectra of glasses at 293 K: (a) phosphorous-based glass KGSS-83; (b) borate glass (67 mol.%  $\text{B}_2\text{O}_3$ , 15 mol.%  $\text{Na}_2\text{O}$ , 18 mol.%  $\text{BaO}$ ); (c) germanate glass (67 mol.%  $\text{GeO}_2$ , 15 mol.%  $\text{Na}_2\text{O}$ , 18 mol.%  $\text{BaO}$ ). Glass composition in (b) and (c) is the same as described in Ref. [75].

High frequency and anharmonicity of OH-oscillations leads to the fact that the impurity of OH-groups in glasses affects quenching kinetics of  $\text{Ln}^{3+}$  luminescence in these media [65–68]. The analysis of deviations of this kinetics from exponential law and comparison of the experimental results with the expectations of dipole-dipole mechanism of nonradiative transitions provided evidence of the dipole-dipole character of electronic-vibrational energy transfer onto OH-oscillations in glasses [66–68].

The d–d mechanism of deactivation for excited  $\text{Ln}^{3+}$  ions on BO-group oscillations was further confirmed by the analysis of quenching kinetics of  $\text{Ln}^{3+}$ -ion luminescence in germanate and phosphate glasses involving BO-group oscillations of higher frequencies [66]. In this case, the calculated nonexponential decay curve for the excited state of  $\text{Ln}^{3+}$  ions in the d–d approximation showed equally good agreement with the experimental data.

The possibility of applying the inductive-resonant theory of nonradiative transitions to low-frequency bases was investigated for the transitions in  $\text{Nd}^{3+}$  ions in fluorozircono-

ate glasses and  $\text{YLiF}_4$  crystals [69, 70], where oscillations of F atoms surrounding Zr and Li are largely responsible for the highest-base vibrational frequency ( $h\nu_{\text{Zr-F}} = 550\text{--}580 \text{ cm}^{-1}$  and  $h\nu_{\text{Li-F}} = 490 \text{ cm}^{-1}$ , respectively). It has been shown that the shape of temperature and energy dependence for linear absorption coefficient  $\alpha(\nu, T)$  of the base is similar to the observed dependence of  $k_{nr}$  on the same parameters (Fig. 4).

**Figure 4.** Comparison of experimentally seen energy (frequency)-dependence of the logarithm of linear absorption coefficient [ $\log \alpha(\nu)$  is the solid line] in fluorozirconate glass [ $\text{ZrF}_4$  (70%),  $\text{BaF}_2$  (16.9%),  $\text{LaF}_3$  (7.6%) and  $\text{NaF}$  (5.4%)] and logarithmic dependence of rate constant for nonradiative transitions from the levels of glass-activating  $\text{Nd}^{3+}$  on the energy gap between this and the nearest lower-lying level [ $\log k_{nr}$  vs.  $\Delta E_{el}$  is denoted by circles] [69].

Similar parallelism between  $k_{nr}(\Delta E)$  and  $k_r \alpha(\Delta E) \nu^{-4}$  dependences for  $\text{YAl}_5\text{O}_{12}$ ,  $\text{YAlO}_3$ ,  $\text{Gd}_3\text{Ga}_5\text{O}_{12}$ ,  $\text{LaP}_5\text{O}_{14}$ ,  $\text{NaLa}(\text{MoO}_4)_2$  crystals was reported in [66]. Using sophisticated experimental techniques, parallelism between changing  $\alpha(\nu)$  of the base and  $k_{nr}$  of rare-earth ions was examined even for single-phonon transitions [53]. In the case of low-frequency bases, reliable prediction of  $k_{nr}$  and their temperature dependence encounters more difficulties due to commensurability between  $\Delta E$  of the transitions being studied and the Stark splitting of interacting levels. For this reason, the

agreement (within one order of magnitude as reported in [69]) between experimental  $k_{\text{nr}}$  and those calculated by the Judd – Ofelt method for certain averaged  $\Delta E$  and taking into account  $k_r$  should be considered as acceptable (Table 7).

**Table 7.** Comparison of nonradiative transition rate constants in  $\text{Nd}^{3+}$  ions in fluorozirconate glasses (at 293 K) obtained in the experiment and calculated with the inductive-resonant theory (from [69])

Transition	$\Delta E_{\text{el}}^{\text{min}}$	$\tau_l, \text{s}$	$k_{\text{nr}}^{\text{exp}}, \text{s}^{-1}$	$k_r, \text{s}^{-1}$	$k_{\text{nr}}^{\text{calc}}, \text{s}^{-1}$
${}^4G_{5/2} + {}^2G_{7/2} - {}^2H_{11/2}$	1000	—	$1.2 \times 10^8$	0.34	$1.3 \times 10^8$
${}^4G_{7/2} + {}^2K_{13/2} - {}^4G_{5/2}$	1270	$2.5 \times 10^{-8}$	$5.7 \times 10^7$	—	—
${}^2P_{3/2} - {}^2D_{5/2}$	2160	$2.1 \times 10^{-5}$	$4.7 \times 10^4$	0.11	$3.4 \times 10^3$
${}^4D_{3/2} - {}^2P_{3/2}$	1750	$4.0 \times 10^{-6}$	$1.8 \times 10^5$	0.13	$1.1 \times 10^4$

Applicability of the d–d approximation in the inductive-resonant theory [70] to  $k_{\text{nr}}$  calculation for  $\text{Ln}^{3+}$  ions in  $\text{YLiF}_4$  crystals is likely to be due to partial localisation of  $\text{LiF}_4$ -group oscillations. Perfect agreement between experimentally obtained  $k_{\text{nr}}$  values for  $\text{Nd}^{3+}$  ions in fluorozirconate glasses and those calculated according to formula (19) suggests that the localisation of highest-frequency oscillations related to the disorganisation of the glassy base [71, 72] allows the inductive-resonant theory in the d–d approximation to be used for calculating  $k_{\text{nr}}$  in  $\text{Ln}^{3+}$  ions in glassy bases undergoing no characteristic oscillations.

Experimental studies [53, 73–77] have shown that  $T$ -dependence of  $k_{\text{nr}}$  for  $\text{Ln}^{3+}$  ions in different bases is described in the high-temperature range by the formula

$$k_{\text{nr}}(T) = k_{\text{nr}}(0) \prod_i (n_i + 1)^{N_i}, \quad (21)$$

where  $k_{\text{nr}}(0)$  is the nonradiative transition rate constant at  $T = 0 \text{ K}$ ,  $n_i = \exp(h\nu_i/kT - 1)^{-1}$ , and  $N_i$  satisfies the condition  $\sum_i N_i h\nu_i = \Delta E_{\text{el}}$ . In systems with a large number of vibrational modes, choice of the number and frequencies of oscillations involved in energy dissipation process for the description of thermal decay is arbitrary. The above formula has been derived for the multifrequency model of electronic excitation energy dissipation. However, it is known from experimental studies that  $T$ -dependence of  $k_{\text{nr}}$  is in most cases well-described by the single-frequency model. If this dependence is to be described in the entire temperature range including the region where  $kT$  is commensurable with the Stark splitting energy, the calculation of  $T$ -dependent  $k_{\text{nr}}$  must be carried out using formula

$$k_{\text{nr}}(T) = k_{\text{nr}}(0) \sum_i \beta_i (n + 1)^{N_i} \exp\left(-\frac{E_i}{kT}\right) 10^{-2E_i/\Gamma} \times \left[ \sum_i \exp\left(-\frac{E_i}{kT}\right) \right]^{-1}, \quad (22)$$

where summation is performed over all Stark sublevels of the upper electronic state;  $E_i$  is the energy of the  $i$ -th sublevel measured from the lowest one;  $N_i$  satisfies the condition  $\Delta E + E_i = N_i h\nu$ ;  $\Gamma = -(1/2) d(\Delta E)/d(\log k_{\text{nr}})$  is the frequency range on which  $k_{\text{nr}}$  changes by two orders of magnitude. Factor  $10^{-2E_i/\Gamma}$  reflects exponential dependence of  $k_{\text{nr}}$  on the energy gap, and the coefficient  $\beta_i = k_{\text{nr}i}/k_{\text{nr}1}$  reflects the dispersion of probabilities for nonradiative transitions from individual Stark sublevels. Experimental  $k_{\text{nr}}$  values for different sublevels may differ by 1–1.5 orders

of magnitude. Therefore, several-fold changes of  $k_{\text{nr}}$  in the low-temperature range ( $kT < \Delta_i$ ) may be due to the altered population of the individual sublevels. The  $k_{\text{nr}}(T)$  dependence shows a characteristic inflection in this temperature range and it is poorly described without taking into account parameters  $\beta_i$  in formula (22). In the  $kT > \Delta_i$  range, the contribution of this factor to the temperature dependence of  $k_{\text{nr}}$  does not exceed 30%. In other words,  $k_{\text{nr}}(T)$  is largely affected by a factor  $(n + 1)^{N_i}$ .

Studies of the temperature effect on the short-wavelength edge of the vibrational absorption spectrum in halide crystals indicate that it exhibits strong temperature dependence [78–80]. Linear absorption coefficient of the base  $\alpha(v)$  grows with increasing temperature according to the law [78]

$$\alpha(v, T) = \alpha(v, 0)(n + 1)^N, \quad (23)$$

where  $n = \exp(h\nu/kT - 1)^{-1}$ ,  $N = \nu/\nu_0$  is the phonon overlapping number (with  $N$  becoming noninteger in the region where vibrational absorptions of adjacent overtones overlap), and  $\nu_0$  is the frequency of average optical phonon. Also, the  $\alpha(v)$  dependence on the phonon overlapping number is known to display exponential-like behaviour [78]. Assuming that the approximation of electrostatic interaction between purely electronic transition in the ion and base oscillations can be used for  $\text{Ln}^{3+}$  ions in any base, there must be a common law for  $k_{\text{nr}}(\Delta E, T)$  and  $\alpha(\Delta E, T)$  dependences, regardless of whether the requirement  $r < R$  (necessary for expansion in multipoles) can be satisfied (see Section 1). It has been noted above that not only  $\Delta E$  and  $T$ -dependences of  $k_{\text{nr}}$  and  $\alpha$  for  $\text{Nd}^{3+}$  and  $\text{Ho}^{3+}$  ions in fluorozirconate glasses and  $\text{YLiF}_4$  crystals are very similar, but also the calculation of  $k_{\text{nr}}$  in the dipole-dipole approximation is correct.

Whenever donor-acceptor oscillations in the course of nonradiative transition process are represented by base oscillations, one should expect symbatic temperature and energy dependence of both  $k_{\text{nr}}$  and linear absorption coefficient of the crystal. However, if deactivation of the ion occurs on local oscillations in its environment, it is exactly this frequency must be present in formula (22). Comparison of temperature dependences for different  $h\nu_{\text{vib}}$  obtained with formula (22) and the corresponding experimental curve  $k_{\text{nr}}(T)$  yields the frequency of the donor-acceptor oscillation responsible for nonradiative transition involved.

The mechanism of  $\text{Er}^{3+}$  and  $\text{Ho}^{3+}$  deactivation in even lower-frequency crystal matrices  $\text{BaY}_2\text{F}_8$ ,  $\text{SrY}_2\text{F}_8$ ,  $\text{SrF}_2$  and  $\text{CaF}_2$  was examined in [70, 79]. Studies in the temperature range of 77–800 K have shown that the dependence  $k_{\text{nr}}(T)$  for multiphonon transitions with any  $\Delta E_{\text{el}}$  in bases with  $h\nu_{\text{vib}} < h\nu_{\text{vib, LaF}}$  is well described at  $h\nu_{\text{vib}} = 350\text{--}360 \text{ cm}^{-1}$  (Fig. 5). This vibrational quantum is apparent in the temperature dependence for the multiphonon absorption wing of the  $\text{LaF}_3$  crystal and determines the shape of  $k_{\text{nr}}(T)$  dependence in  $\text{Ln}^{3+}$  ions in the given crystal [70, 79].

This result suggests that nonradiative transitions in fluoride bases with  $h\nu_{\text{vib, base}} < h\nu_{\text{vib, LnF}}$  occur due to the interaction between electronic transition in the ion and quasi-local oscillations of a given  $\text{LnF}_3$  centre. Hence, in bases with the threshold quantum below the corresponding  $\text{Ln}_m\text{X}_n$  quantum, where  $\text{X} = \text{F}, \text{Cl}, \text{S}, \text{O}$ , and  $\text{Br}$ , it makes no sense to use data on the phonon density of the base or its  $\alpha(v)$  in the calculation of  $k_{\text{nr}}$  for  $\text{Ln}^{3+}$  ions. To this effect it is necessary to draw on  $\alpha(v, T)$  for the corresponding base of  $\text{Ln}_m\text{X}_n$ .

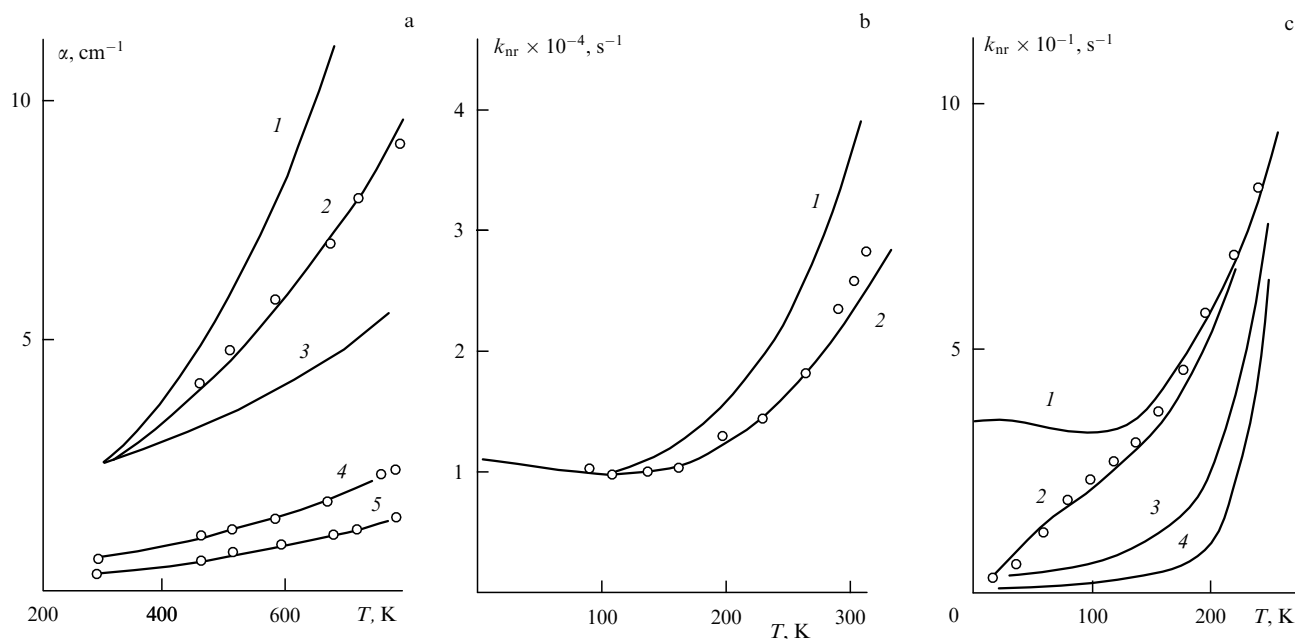


**Figure 5.** The choice of vibrational quantum ( $h\nu_{\text{vib}}$ ) determining  $T$ -dependences of  $\alpha(T)$  for  $\text{LaF}_3$  crystal and  $k_{\text{nr}}$ . Experimental and theoretical results are denoted by circles and solid lines, respectively. (a)  $\alpha(T)$  dependence: 1, 2, 3 — for absorption at  $950\text{ cm}^{-1}$ , 4 — at  $1080\text{ cm}^{-1}$ , 5 — at  $1130\text{ cm}^{-1}$ ; 1 — calculation of  $\alpha(T)$  using formula (23) when  $h\nu_{\text{vib}} = 300\text{ cm}^{-1}$ , 3 —  $h\nu_{\text{vib}} = 470\text{ cm}^{-1}$ , 2, 4, 5 —  $h\nu_{\text{vib}} = 360\text{ cm}^{-1}$ . (b) 1 — calculation of  $k_{\text{nr}}(T)$  for the  ${}^2H_{9/2} - {}^4F_{3/2}$  transition in  $\text{Er}^{3+}$  in  $\text{LaF}_3$  crystal when  $h\nu_{\text{vib}} = 310\text{ cm}^{-1}$ , 2 — experimental [70] and calculated curves for the same transition with the choice of  $h\nu_{\text{vib}} = 360\text{ cm}^{-1}$ . (c) Circles are experimental data on  $k_{\text{nr}}(T)$  of the  ${}^4S_{3/2} - {}^4F_{9/2}$  transition in  $\text{Er}^{3+}$  in a  $\text{BaF}_2$  crystal [79] and calculated curves apply to  $h\nu_{\text{vib}} = 360\text{ cm}^{-1}$ ,  $\beta_2 = 1$  (1),  $h\nu_{\text{vib}} = 360\text{ cm}^{-1}$ ,  $\beta_2 = 50$  (2),  $h\nu_{\text{vib}} = 250\text{ cm}^{-1}$ ,  $\beta_2 = 1$  (3), and  $h\nu_{\text{vib}} = 188\text{ cm}^{-1}$ ,  $\beta_2 = 1$  (4).

To sum up, experimental studies indicate that, regardless of the base of  $\text{Ln}^{3+}$  ions, it is valid to use the approximation of the interaction between the purely electronic oscillator of ion transition and the highest-frequency oscillations in the ion's environment. It is therefore possible to calculate Franck–Condon factors of corresponding nonradiative transitions in  $\text{Ln}^{3+}$  ions in any base through the overlap integral over the emission spectrum of the transition in question and the spectrum of vibrational absorption in this transition region. The agreement between theoretical and experimental  $k_{\text{nr}}$  values within an order of magnitude as reported in this section appears to confirm the applicability of the dipole-dipole approximation of the inductive-resonant theory to the calculation of  $k_{\text{nr}}$  for  $\text{Ln}^{3+}$  ions in glasses and various crystals. This is true because the reliability of some parameters used in  $k_{\text{nr}}$  computation is significantly smaller for these bases as compared to solutions.

The reduced accuracy of calculations can be accounted for by the fact that transitions in these bases occur between high excited levels in the range of energy gaps  $\Delta E_{\text{el}} = 1500 - 3000\text{ cm}^{-1}$ . In this range neither spectra nor probabilities of radiative transitions have been measured and calculations are carried out using spectra obtained from Stark splitting studies, without taking into account intensity distribution over individual Stark components. In the case discussed, the averaged  $k_{\text{r}}$  was calculated by the Judd–Ofelt method instead of  $k_{\text{r}}$  values for transitions between individual Stark sublevels. The choice of  $\Delta E_{\text{el}}$  to calculate spectrum overlapping was equally unreliable.

Taken together, these arguments account for the reduced accuracy of calculated results for  $k_{\text{nr}}$  as compared with those in solutions, for which experimental parameters (spectra,  $k_{\text{r}}$ ) can be used in calculating  $k_{\text{nr}}$ .

### 3.2 Ions of transition metals in solutions, glasses and crystals

Mechanisms underlying nonradiative transitions in ions of transition metals (TM) have been discussed in several reviews and monographs [80, 81]. The growing interest in photophysics of TM ions is largely due to their basic role in lasers tuned over a wide spectral range [82].

Unlike trivalent lanthanides, TM ions show conspicuous tendency to be involved in electron transfer. Due to this, excited states of TM ions are more frequently deactivated through the ‘chemical mechanism’. For this reason, the physical nature of nonradiative transitions must be confirmed if the applicability of the inductive-resonant mechanism of deactivation of such ions is to be elucidated [83]. Another difficulty encountered in the analysis of mechanisms of nonradiative transitions in TM ions is that the lowest excited state in TM complexes is usually the charge transfer state or a state of other configuration. Although such a state is sometimes luminescent, it is impossible to speak about its localisation inside the  $d$ -shell of the ion. Moreover,  $d$ -electrons of TM ions tend to interact stronger with ligand orbitals and markedly change their properties upon excitation. This explains why in certain transitions TM ions, unlike  $\text{Ln}^{3+}$ , are characterised by well-developed vibronic spectra, that is, their spectra reflect ‘moderate’ or even ‘strong’ vibronic coupling [84].

The scheme of energy levels which illustrates nonradiative deactivation through the inductive-resonant mechanism in TM ions with well-developed vibronic spectra is presented in Fig. 6. Energy resonance in TM ions, unlike that in  $\text{Ln}^{3+}$ , is largely due to vibronic levels of the ion. A fraction of energy spent on donor-acceptor oscillations of atomic groups in the base depends on the strength of vibronic coupling, anharmonic

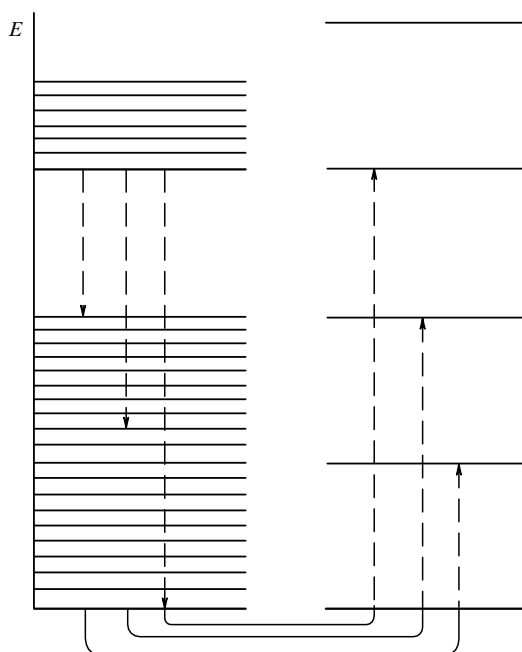


**Figure 6.** Level scheme illustrating the inductive-resonant theory of nonradiative transitions as applied to transition metal ions. Electronic levels of a transition metal ion are shown on the left-hand side (bold lines) and vibronic levels, on the right-hand side (thin lines). Vibrational levels of donor-acceptor oscillations of ligands and solvent molecules are presented on the right-hand side (thin lines). Vertical dashed lines denote nonradiative energy transfer responsible for nonradiative transitions with excitation of acceptor oscillations in the ion and donor-acceptor oscillations in the ion's environment.

nicity and frequency of oscillations involved in energy dissipation. Evidently, the contribution of donor-acceptor oscillations of the base to nonradiative transitions grows with increasing their frequencies and anharmonicity and decreasing an ion heat release.

Experimental verification of the applicability of the inductive-resonant theory to TM ions was accomplished using complexes  $\text{Cr}^{3+}$  [85–87],  $\text{Mn}^{2+}$  [88–91],  $\text{V}^{4+}$  [92], and  $\text{Ru}^{2+}$  [93]. We consider a study on nonradiative transition mechanisms in TM ions to be of special importance because some authors who recognise the validity of the inductive-resonant theory of nonradiative transitions [3, 5, 7] argue that it is applicable only to weak vibronic coupling. On the contrary, we have always maintained [4] that this theory may be applied to a much broader group of luminescent systems, specifically to TM ions regardless of the strength of vibronic coupling in transitions.

Observed phosphorescence of  $[\text{Cr}(\text{NCS})_6]^{3-}$ ,  $[\text{Cr}(\text{en}-h_4)_3]^{3+}$ ,  $[\text{Cr}(\text{en}-d_4)_3]^{3+}$ ,  $[\text{Cr}(\text{NH}_3)_6]^{3+}$ ,  $[\text{Cr}(\text{ND}_3)_6]^{3+}$ ,  $[\text{Cr}(\text{NH}_3)_2(\text{NCS})_4]^-$ ,  $[\text{Cr}(\text{ND}_3)_2(\text{NCS})_4]^-$  complexes, in which  $\text{Cr}^{3+}$  is coordinated via nitrogen, is believed to be largely due to the intercombination transition  ${}^2E_g - {}^4A_{2g}$  localised on  $\text{Cr}^{3+}$  [85, 86]. Marked effect of solvent deuteration in the case of  $[\text{Cr}(\text{NCS})_6]^{3-}$  and/or ligand deuteration for all other complexes has been demonstrated. The effect was especially pronounced when the  $[\text{Cr}(\text{NH}_3)_6]^{3+}$  complex was substituted by its deuterated analog (Table 8), due to the high frequency and strong anharmonism of N–H valent oscillation and close resonance between the  $\text{Cr}^{3+}$  luminescence spectrum and the fourth overtone of NH-oscillations.

**Table 8.** Effect of ligand and solvent deuteration on the phosphorescence quenching time of  $\text{Cr}^{3+}$  complexes ( ${}^2E_g - {}^4A_{2g}$  transition) at 77 K (from [85, 86])

Complex	Solvent	$\tau_{\text{ph}}^{\text{exp}}$	$\tau_{\text{ph}}^{\text{calc}}$
$[\text{Cr}(\text{NH}_3)_6](\text{NO}_3)_3$	$(\text{CH}_3)_2\text{SO}$	54	—
	$\text{CH}_3\text{OH} + \text{H}_2\text{O}$ (2 : 1)	54	—
$[\text{Cr}(\text{ND}_3)_6](\text{NO}_3)_3$	$\text{CD}_3\text{OD} + \text{D}_2\text{O}$ (2 : 1)	4350	—
$[\text{Cr}(\text{en}-h_4)_3](\text{ClO}_4)_3$	$\text{CH}_3\text{OH}$	110	140
	$(\text{CH}_3)_2\text{SO}$	110	—
$[\text{Cr}(\text{en}-d_4)_3](\text{ClO}_4)_3$	$\text{CD}_3\text{OD}$	4350	—
$[\text{Cr}(\text{NH}_3)_2(\text{NCS})_4]\text{NH}_4$	$\text{CH}_3\text{OH}$	430	—
$[\text{Cr}(\text{ND}_3)_2(\text{NCS})_4]\text{ND}_4$	$\text{CD}_3\text{OD}$	2800	—
$[\text{Cr}(\text{NCS})_6]\text{K}_3$	$\text{H}_2\text{O}$	2000	6000
	$\text{D}_2\text{O}$	9000	19000
	$\text{CH}_3\text{OH}$	8500	9500
	$\text{CD}_3\text{OD}$	25000	—
$[\text{Cr}(\text{NCS})_5\text{CH}_3\text{OH}]\text{K}_2$	$\text{CH}_3\text{OH}$	550	—
$[\text{Cr}(\text{NCS})_5\text{CD}_3\text{OD}]\text{K}_2$	$\text{CD}_3\text{OD}$	7400	—

Also, it has been demonstrated that the role of the solvent in the degradation of excitation in  $\text{Cr}^{3+}$  is quite different in hexarhodanide and amine complexes. The quenching time  $\tau_{\text{ph}}$  of  $[\text{Cr}(\text{NCS})_6]^{3-}$  phosphorescence varies broadly not only in protonated but also in deuterated solvents. At the same time, for  $\text{Cr}^{3+}$  complexes containing N–H and N–D groups in the inner coordination sphere  $\tau_{\text{ph}}$  is wholly determined by the probability of electronic energy dissipation on the nearest N–H(D) oscillations. It has been shown [87] that the low deactivating power of  $\text{N}\equiv\text{C}$  valent oscillations in  $\text{NCS}^-$  anion ( $\nu = 2080 \text{ cm}^{-1}$ ) is due to a small anharmonicity as compared with N–H(D), O–H(D), and C–H(D) oscillations. Measurements on IR absorption spectra of  $\text{NCS}^-$  anion indicate that the ratio of intensity of the first overtone of the  $2080 \text{ cm}^{-1}$  band to that of the main band is one order of magnitude smaller than the intensity ratio for C–D oscillations ( $\nu = 2230 - 2255 \text{ cm}^{-1}$ ). For this reason, the nonradiative transition rate in  $[\text{Cr}(\text{NCS})_6]^{3-}$  complexes depends not so much on the rhodanide ion immediately adjacent to  $\text{Cr}^{3+}$  as on the more distant O–H(D) or C–H(D)-groups of the solvent. This situation is very much like that with  $\text{Ln}^{3+}$ -acetonitrile complexes as described in the previous section.

We have earlier emphasised that the necessity to take into account vibronic structure of the luminescence spectrum in  $k_{\text{nr}}$  calculation grows with the increased strength of vibronic coupling. This prediction is possible to confirm using the divalent ion of manganese. Luminescence spectra of  $\text{MnHal}_2$  are located in the  $17000 - 10000 \text{ cm}^{-1}$  region and correspond to the intercombination  ${}^4T_1 - {}^6A_1$  transition accompanied by a marked shift of adiabatic potential upon excitation [84]. Sell et al. [91] have shown that the luminescent  ${}^4T_1 - {}^6A_1$  transition is essentially the electric dipole one while strong effect of deuteration suggests the physical mechanism of nonradiative transitions.

Table 9 summarises measured values of the luminescence quenching time  $\tau_1^{\text{exp}}$  as compared to  $\tau_1^{\text{calc}}$  values calculated with the inductive-resonant theory for  $\text{Mn}^{2+}$  ions in different environments. Evidently, there is a good agreement between theoretical and observed  $\tau_1$  values. Noteworthy is a marked decrease in  $\tau_1$  on passing from frozen to pumped-out liquid solution. Strong thermal quenching of luminescence is achieved either through the electron transfer mechanism or via crossing of two markedly displaced potential surfaces of the excited and ground states. At the same time, thermal

**Table 9.** Comparison of the observed luminescence quenching time  $\tau_1^{\text{exp}}$  for  $\text{Mn}^{2+}$  ( ${}^4T_1$ ) ions in various media and at different temperatures with  $\tau_1^{\text{calc}}$  calculated in the framework of the inductive-resonant theory (octahedric environment, oxygen-free solutions) (from [88, 90, 94])

Compound	Solvent	$k_r, \text{s}^{-1}$		$\tau_1^{\text{exp}}, \mu\text{s}$		$\tau_1^{\text{calc}}, \mu\text{s}$	
		295 K	77 K	295 K	77 K	295 K	77 K
$\text{MnCl}_2$	$\text{H}_2\text{O}$	105	48	5.3	42	6.1	63
	$\text{D}_2\text{O}$	105	48	45	1250	210	1500
$\text{MnCl}_2 \cdot 4\text{H}_2\text{O}$	Crystal	105	—	46	75	51	—
$\text{MnCl}_2 \cdot 4\text{D}_2\text{O}$	Crystal	105	—	660	1800	1800	—
$\text{MnBr}_2$	$\text{H}_2\text{O}$	230	106	4.5	35	6.0	57
	$\text{D}_2\text{O}$	230	106	56	1200	250	1250
$\text{MnBr}_2 \cdot 4\text{H}_2\text{O}$	Crystal	230	—	43	75	58	—
$\text{MnBr}_2 \cdot 4\text{D}_2\text{O}$	Crystal	230	—	530	1400	1000	—
$\text{MnCl}_2$	$\text{CH}_3\text{OH}$	100	36	10	60	12	70
	$\text{CD}_3\text{OD}$	100	36	120	2200	300	2300
$\text{MnBr}_2$	$\text{CH}_3\text{OH}$	230	100	12	80	12	110
	$\text{CD}_3\text{OD}$	230	100	150	3000	360	4000

quenching of luminescence in  $\text{Mn}^{2+}$ -salt solutions in water or methanol can be equally well accounted for in the context of the inductive-resonant theory. In the case of strong vibronic coupling, nonradiative transitions involve low-frequency Mn–O oscillations whose filling in the temperature range from 77 to 300 K shows temperature dependence. Hence,  $k_{\text{nr}}$  must also depend on temperature if the physical mechanism of nonradiative transitions is operative. Not surprisingly, taking into consideration changes of the overlap integral over the luminescence spectrum of  $\text{Mn}^{2+}$  and the vibrational absorption spectrum of water completely explains the observed  $\tau_1$  variations for  $\text{Mn}^{2+}$  in the temperature range from 77 to 295 K (see Table 9).

The difference in overlap integrals over spectra also accounts for the marked discrepancy between  $k_{\text{nr}}$  values for  $\text{Mn}^{2+}$  halide salts in solutions and in  $\text{MnCl}_2$  and  $\text{MnBr}_2$  crystallohydrates, which we have found in an earlier study. In the case of  $\text{Mn}^{2+}$ , there is also strong dependence of  $k_{\text{nr}}$  on the distance between the electronic excitation centre ( $\text{Mn}^{2+}$  in the  ${}^4T_1$  state) and the molecular groups showing donor-acceptor oscillations (e.g. C–H<sub>n</sub> groups). Similar to the case of  $\text{Yb}^{3+}$  (see Table 2 above),  $k_{\text{nr}}$  is inversely proportional to the third power of the distance to high-frequency C–H-oscillations which induce nonradiative transitions. This makes the interaction between electric dipoles sufficient for the  $k_{\text{nr}}$  calculation. True, the altered environment of  $\text{Mn}^{2+}$  results in significant changes of both the luminescence spectrum (hence, the overlap integral over spectra) and the emission rate constant, unlike the situation with  $\text{Yb}^{3+}$  and  $\text{Dy}^{3+}$  ions where neither the radiative constant, nor the overlap integral over spectra of  $\text{Ln}^{3+}$  luminescence and vibrational absorption exhibits marked dependence on environmental changes.

It follows from formulas (18), (19) that quantity  $k_{\text{nr}}a^3/(k_r \int_{\text{ov}})$  for TM ions (see formula (19) for notation) must be constant whereas in the case of the dipole-dipole approximation for  $\text{Ln}^{3+}$  ions it is the product  $k_{\text{nr}}a^3$  that remains constant ( $a$  is the sphere surrounding the excited ion in which the donor-acceptor oscillations are absent). Indeed, our calculations based on experimental findings [88] indicate that the above quantity remains unaltered to within 30% although the  $k_{\text{nr}}$  value of  $\text{Mn}^{2+}$  ion undergoes a 52-fold change when passing from  $\text{CH}_3\text{OD}$  to  $(\text{C}_3\text{H}_7\text{O})_3\text{PO}$  (see Table 10).

Another object for which the applicability of the inductive-resonant theory has been confirmed is the  $\text{V}^{4+}$  ion in

**Table 10.** Dependence of the rate constant of nonradiative transitions from the  ${}^4T_{1g}$ -level of  $\text{Mn}^{2+}$  (octahedric configuration) in  $\text{MnCl}_2$  solutions at 77 K on the distance to donor-acceptor  $\text{CH}_n$  groups (from [88])

Solvent	$a, \text{\AA}$	$k_{\text{nr}}, \text{s}^{-1}$	$k_r, \text{s}^{-1}$	$\int_{\text{ov}}, \text{abs. units}$	$\frac{k_{\text{nr}}a^3}{k_r \int_{\text{ov}}}$	$\tau_1^{\text{exp}}, \mu\text{s}$	$\tau_1^{\text{calc}}, \mu\text{s}$	$\nu_1^{\text{max}}, \text{cm}^{-1}$
$\text{H}_2\text{O}$	2.0	$2.9 \times 10^4$	36	15.0	—	35	42	13800
$\text{CH}_3\text{OH}$	2.0	$1.7 \times 10^4$	36	9.2	—	60	70	13800
	3.43							
$\text{CH}_3\text{OD}$	3.43	$1.2 \times 10^3$	36	6.8	7.1	850	1900	13800
$(\text{CH}_3)_2\text{SO}$	4.3	$3.8 \times 10^2$	42	3.1	9.9	2400	7500	14500
$(\text{C}_4\text{H}_9\text{O})_3\text{PO}$	6.0	21	42	0.54	9.2	17000	23000	16000

solutions at 77 K. Transition  ${}^2E(t_{xz, yz}) - {}^2B(t_{xy})$  of  $\text{V}^{4+}$  ion is located in the near IR region; its luminescence spectrum is formed by V=O oscillations ( $800 \text{ cm}^{-1}$ ) with the heat release parameter  $\gamma^2 = 0.9$  [92]. Table 11 presents quantum yields  $q_1$  of  $\text{V}^{4+}$  luminescence in different solutions calculated with the inductive-resonant theory and found in the experiment. As indicated by the table, there is good agreement between the observed and theoretical values. The calculation of luminescence quantum yields is convenient in that it does not require knowing  $k_r$  values because  $q_1 = k_r/(k_r + k_{\text{nr}})$  while  $k_{\text{nr}}$  is proportional to  $k_r$ , in accordance with formulas (18), (19). Hence,  $k_r$  in expression for  $q_1^{\text{calc}}$  cancels.

**Table 11.** Comparison between quantum yields  $q_1$  of  $\text{V}^{4+}$  luminescence in  $\text{VOCl}_2$  solutions at 77 K obtained in the experiment and calculated from the inductive-resonant theory (from [92])

Solvent	$q_1^{\text{exp}}$	$q_1^{\text{calc}}$	$\tau_1^{\text{exp}}, \mu\text{s}$
$\text{C}_2\text{H}_5\text{OH}$	—	$5 \times 10^{-4}$	<0.02
$\text{C}_2\text{D}_5\text{OD}$	$1.0 \times 10^{-2}$	$1.0 \times 10^{-2}$	0.75
$\text{C}_2\text{D}_5\text{OD} + \text{KNCS}$	$6.0 \times 10^{-2}$	—	3–4
$(\text{C}_3\text{H}_7\text{O})_3\text{PO}$	$> 8 \times 10^{-3}$	$2.0 \times 10^{-2}$	1.5
$(\text{C}_3\text{D}_7\text{O})_3\text{PO}$	$2.2 \times 10^{-1}$	$3.5 \times 10^{-1}$	30

Analysis of temperature dependence of the luminescence decay time for  $\text{Ru}(\text{bpy})_3^{2+}$  complexes in solutions confirmed proportionality between  $k_{\text{nr}}$  and  $k_r$  ensuing from the inductive-resonant theory (see formulas (18), (19)). Luminescence of the tris-bipyridyl complex of ruthenium was shown to be consistent with the intercombination transition from the excited triplet state to the singlet ground state with electron transfer from  $\text{Ru}^{2+}$  to one of the bipyridyl ligands. The phosphorescence decay time of  $\text{Ru}(\text{bpy})_3^{2+}$  was found to grow rapidly with a decrease in temperature [94–96]; the increase is especially pronounced at low temperatures (2.1–10 K) [94]. Phosphorescence spectra and quantum yields in the same temperature range are practically unaltered. The same is true of the vibrational absorption spectra of bipyridyl ligands and solvent molecules surrounding the complex. These facts can be explained on the assumption of proportionality between rate constants of radiative and nonradiative transitions. This provides further evidence of the validity of the inductive-resonant theory. At the same time, the lack of parallelism in  $k_r$  and  $k_{\text{nr}}$  changes reported by certain authors cannot be regarded as an argument against validity of this theory. It has been shown in [94] that the absence of parallelism in the removal of the spin forbiddenness on  $k_r$  and  $k_{\text{nr}}$  values in  $\text{Mn}^{2+}$  halogenide solutions by heavy atoms (Cl, Br, J) can be explained in terms of the inductive-resonant theory taking into account (through the overlap integral over spectra) effect of these anions on the shape of the manganese luminescence spectrum. The use of the inductive-resonant

theory in  $k_{nr}$  calculations allows its changes (experimentally seen at the salt anion replacement) to be correctly predicted. Thus, the inductive-resonant theory explains not only proportionality between  $k_r$  and  $k_{nr}$  observed in the experiment but also its absence.

Similarly, the inductive-resonant theory can be employed to explain the marked discrepancy reported in [97] between  $q_1$  values for  $V^{3+}$  ions in crystals differing in symmetry of the immediate ion environment. Symmetry lowering in the centre is known to result in splitting of the low-lying  ${}^3T_1$ -level of  $V^{3+}$  ions. This leads not only to a change in  $\Delta E_{el}$  relating to the excited and the nearest unexcited levels but also to the altered luminescence spectrum [98]. Specifically, the narrow-band spectrum undergoes transformation to a spectrum of two bands, with the half-width of the long-wavelength band being  $\sim 1000 \text{ cm}^{-1}$  which suggests large heat release parameter [98]. According to the inductive-resonant theory, such spectral change should result in a significant growth of the overlap integral over spectra, hence in markedly increased  $k_{nr}$  of the transition.

Such splitting of the ion's ground state with the symmetry lowering in its immediate environment may be a cause of decreased  $q_1$  of TM ions in going from crystal bases to glasses [99] in which the symmetry of centres is usually lowered. Another cause is the decreased strength of the crystal field and the inhomogeneous environment of ions in glasses.

Analysis of luminescence, absorption, and excitation spectra of  $Cr^{3+}$  [100],  $V^{4+}$  [101],  $Mo^{3+}$  [102],  $Mo^{5+}$  [103], and  $Cu^+$  [83] ions in glasses has demonstrated their markedly inhomogeneous broadening; this is especially true of the absorption spectra. Inhomogeneity of the ensemble is also evidenced by the lack of exponential luminescence quenching of these ions in glasses. It has been shown in an earlier study [83] that the analysis of dependence of the time  $\tau_1^e$  of an  $e$ -fold decrease in luminescence intensity on  $\lambda_{obs}$  allows the nature of ion deactivation to be elucidated. When deactivation occurs through the physical mechanism,  $\tau_1$  falls as  $\lambda_{obs}$  shifts towards the long-wave part of the spectrum (in accordance with the law of  $k_{nr}$  dependence on  $\Delta E_{el}$ ). Such dependence of  $\tau_1^e$  on  $\lambda_{obs}$  is known for  $V^{4+}$ ,  $Mo^{5+}$ , and  $Mo^{3+}$  ions in glasses and confirms the physical mechanism of their deactivation. A study of  ${}^2E - {}^2B_2$  nonradiative transitions of  $V^{4+}$  ions in phosphate and composite boron-fluorophosphate glasses [101] has shown that inhomogeneous ensembles gave rise to centres with  $k_{nr}$  values differing by one or two orders of magnitude; besides, these glasses contained a certain amount of centres for which  $q_1 = 1$ . Luminescence spectra of TM ions undergoing stationary excitation are dominated by centres with highest luminescence yields. For this reason, estimates of luminescence yields of TM ions based on  $k_r$  values and  $k_{nr}$  calculated with the help of formula (19) taking into account the observed luminescence spectrum are close to the upper limit of  $q_1$  for TM ions in these glasses. Naturally, the higher the degree of inhomogeneity in the broadening of absorption spectra, the greater the difference between estimated and observed  $q_1$  values. Measurements of  $q_1$  for  $V^{4+}$  ions in barium metaphosphate were made in [79]. The luminescence yield in this glass was found to be 0.0025 and 0.025 at 77 K and 300 K, respectively. And quenching of luminescence was non-exponential. Calculation of  $k_{nr}$  using formula (19) required extrapolation of  $V^{4+}$  luminescence spectrum to the region of fundamental tone oscillations of PO-groups in the matrix which was a source of additional error. Nevertheless, the calculated  $q_1$  value turned out to be only an order of

magnitude higher than the observed one. It was concluded that formula (19) may be used to calculate  $q_1$  of TM ions implanted to glasses.

### 3.3 Molecules in the condensed phase

**3.3.1 Oxygen.** The lower excited state of the oxygen molecule is the  ${}^1\Delta_g$  state. Oxygen being of paramount importance for photochemical and biological processes, its lifetime in various solvents and mechanism of deactivation have been studied by many authors [104–108]. Schmidt [109] has demonstrated that deactivation of electronic excitation for the  ${}^1\Delta_g$  state of oxygen molecule occurs as a result of interaction between electronic oscillator and selected vibrational oscillator. The  $\tau_1$  of the  ${}^1\Delta_g$  state was found to increase 30 times on following successive substitution of CH-oscillations by CD- and CF-oscillations. The difference between  $\tau_1$  values for the  ${}^1\Delta_g$  state of oxygen molecules in  $H_2O$  and  $C_2F_3Cl_3$  exceeded four orders of magnitude. Taken together, experimental findings [109] indicate that nonradiative deactivation of the  ${}^1\Delta_g$  state is due to electronic-vibrational energy transfer even though the mechanism of this process remains a matter of dispute. Merkel and Kearns [110] were the first to carry out experiments which provided a deeper insight into the mechanism of deactivation of the singlet excited state of oxygen. These authors observed marked effect of deuteration of hydrogen-containing solvents on the  ${}^1\Delta_g$  state quenching time and confirmed the previously known increase in  $\tau_1$  of the  ${}^1\Delta_g$  state in solvents containing no hydrogen and, consequently, high-frequency oscillations. They also measured linear absorption coefficients  $\alpha(\nu)$  of the solvents in two short-wavelength luminescence bands of singlet oxygen and provided data on  $\tau_1$  and linear absorption coefficients  $\alpha(\nu)$  of the solvents. These data were shown to correlate, which is consistent with the inductive-resonant mechanism of the  ${}^1\Delta_g - {}^3\Sigma_g^-$  nonradiative transitions in these systems.

In compliance with formulas (18), (19), there is a good agreement between the predicted and observed  $k_{nr}$  ratios in H- and D-containing solvents as well as the correlation between the observed variations of  $k_{nr}$  ( $\tau_1$ ) and overlap integrals. However, calculation of the absolute  $k_{nr}$  value according to the Galanin–Frank formula (19) and using quantity  $k_r$  for the  ${}^1\Delta_g - {}^3\Sigma_g^-$  transition in solvents ( $k_r = 1.3 \text{ s}^{-1}$  [109]) at  $a = 0.33 \text{ nm}$  yields  $k_{nr}$  which is two or three orders of magnitude lower than the observed value.

We have noted in Section 3.1 that radiative and non-radiative transitions may be of different nature especially in the case of magnetic-dipole transitions. It is known from the experience that the  $a {}^1\Delta_g - X {}^3\Sigma_g^-$  transition shows a magnetic-dipole nature with quadrupole impurity. Bearing this in mind, we estimated the contribution of the electric-quadrupole component to this radiative transition [111] and calculated  $k_{nr}$  using formula for the quadrupole-dipole transition [44] that follows:

$$k_{nr} = \frac{9k_r^{eq}}{32\pi^6 n^6 a^5} \int I_1^n(\nu) \alpha(\nu) \nu^{-6} d\nu, \quad (24)$$

where  $I_1^n(\nu)$  is the normalised oxygen emission spectrum;  $\alpha(\nu)$  is the coefficient of linear vibrational absorption of the solvent;  $k_r^{eq}$  is the radiative constant of the admixture of quadrupole transition into the  $a {}^1\Delta_g - X {}^3\Sigma_g^-$  transition;  $a$  is the radius of the initial non-absorbing sphere around the ion, and  $n$  is the refractive index of the medium.



Comparison of theoretical and experimental results shows a good agreement between the two sets of data (Table 12).

**Table 12.** Comparison of  ${}^1\Delta_g - X^3\Sigma_g^-$  nonradiative transition rate constants for the oxygen molecule in solution at 293 K observed in the experiment and calculated using formula (24)

Solvent	$k_{nr}^{exp}, s^{-1}$			$k_{nr}^{calc}, s^{-1}$
	[110]	[112]	[109]	[111]
H <sub>2</sub> O	$3.0 \times 10^5$	$5.0 \times 10^5$	$2.4 \times 10^5$	$1.2 \times 10^5$
C <sub>2</sub> H <sub>5</sub> OH	$1.0 \times 10^5$	$8.3 \times 10^4$	—	$3.0 \times 10^4$
D <sub>2</sub> O	—	$5.0 \times 10^4$	$1.5 \times 10^4$	$1.0 \times 10^4$
(C <sub>2</sub> H <sub>5</sub> ) <sub>2</sub> O	$2.8 \times 10^4$	—	—	$4.0 \times 10^4$
CH <sub>3</sub> (CH <sub>2</sub> ) <sub>4</sub> CH <sub>3</sub>	$3.3 \times 10^4$	—	—	$1.5 \times 10^4$
C <sub>6</sub> H <sub>6</sub>	$3.3 \times 10^4$	—	$3.3 \times 10^4$	$7.0 \times 10^3$
CHCl <sub>3</sub>	$4.0 \times 10^3$	$1.7 \times 10^4$	—	$2.5 \times 10^2$

To summarise, the downward nonradiative transitions in H- and D-containing solvents for oxygen molecules in the  ${}^1\Delta_g$  state is determined by the interaction of the electric quadrupole component of radiative transition between  ${}^1\Delta_g$  and  ${}^3\Sigma_g^-$  states with electric dipole of vibrational transitions. It may be inferred that  $k_{nr}$  values in solvents with lower limiting frequency and smaller anharmonicity would depend on interaction between vibrational oscillators of the medium and the vibronic, rather than electronic, oscillator of the transition.

**3.3.2 Organic molecules.** The mechanisms of nonradiative transitions in complex polyatomic organic molecules are even more versatile than in metal ions and simple molecules. A large number of monographs [2, 3, 6] and reviews [113, 114] have been devoted to photophysics of organic molecules. As before, we shall confine ourselves to ‘physical’ nonradiative transitions and examine only nonradiative transitions between the low triplet and unexcited singlet levels of organic molecules because a major feature of the ‘physical’ mechanism of deactivation is the deuteration effect which was first reported in [115] and afterwards examined many times in relation to the phosphorescence decay time of aromatic compounds. Effects of molecular deuteration on their  $\tau_{ph}$  have been reviewed in [4]. In the majority of luminescent molecules for which it is easy to determine constants of radiative and nonradiative transitions between low-excited levels  $S_1$ ,  $T_1$ , and  $S_0$  (see the scheme of levels in Fig. 7), the  $T_1 - S_0$  nonradiative transition is most frequently proceeded through the ‘physical’ mechanism. This does not refer to molecules undergoing photoisomerization via the stilben-like triplet state in a liquid solution [116]. Moreover, there are normally no intermediate levels between the  $S_0$  and  $T_1$  ones while they do exist between  $T_1$  and  $S_1$ , and higher levels even though their exact positions are unknown. It is expected that the extension of experience at nonradiative transition studies in metal ions in solutions to complex organic molecules may reveal the following patterns of nonradiative transitions in these structures. First, reduced frequency of donor-acceptor oscillations (substitution of CH by CD, CF, and CCl must result in smaller  $k_{nr}$ ). Second, replacement of hydrogen atoms in aromatic rings by substitutes containing XH-groups and located farther apart from these rings than CH-groups, must also lead to smaller  $k_{nr}$ . Third, there must be linear  $\Delta E_{el}$ -dependence of  $\log k_{nr}$  in a series of related compounds, and the condition of direct proportionality between  $k_{nr}$  and the overlap integral over spectra must be fulfilled for all the

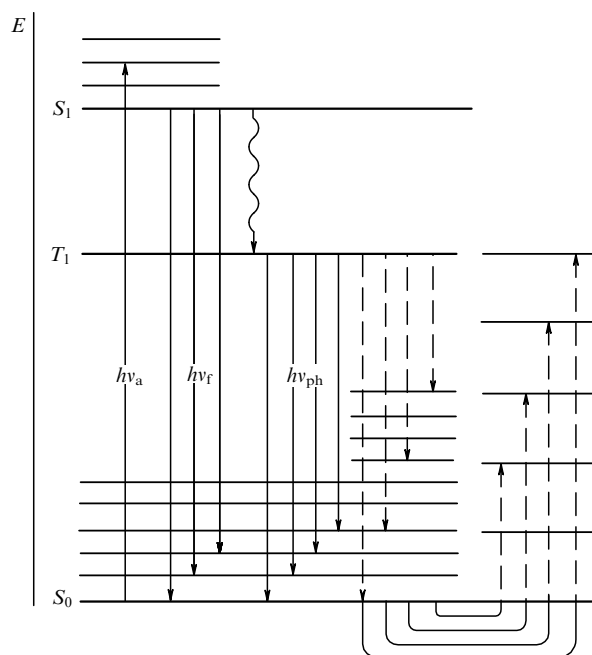


**Figure 7.** Diagrammatic of levels illustrating the inductive-resonant theory of nonradiative transitions from the low-excited triplet level of an organic molecule ( $T_1$ ) to the ground level ( $S_0$ ). Bold lines are electronic levels, thin lines are vibronic and vibrational levels. The left-hand side of the scheme represent electronic and vibronic levels of the molecule excited upon electronic transition (e.g. C–C-skeletal oscillations, C=O-valent oscillations, etc. referred to in the present paper as acceptor oscillations). The right-hand side shows levels of highest-frequency strongly anharmonic oscillations of the molecule or the nearest neighbours (C–H(D), O–H(D), N–H(D)) which we call donor-acceptor oscillations. Vertical dashed lines denote electronic-vibrational energy transfer (nonradiative transition).

compounds regardless of the choice of perturbation operator. If the dipole-dipole approximation is valid,  $k_{nr}$  must change in proportion to  $k_r \int I_r^n(v) \epsilon_{vib}(v) v^{-4} dv$ .

What are the major patterns of nonradiative transitions observed in the experiment? It is known [4] that for  $\Delta E_{el} \gg hv_{XH}$ , deuteration of XH (where X=C, N, O) always leads to decreased  $k_{nr}$ . At the same time, substitution of F or Cl for H [117] does not result in a decrease of  $k_{nr}$ . It is also known from [118] that  $k_{nr}$  decreases with increasing distance between CH-groups and site of the electronic excitation localisation whereas deuteration of different CH-groups in the ring has a variable effect on  $k_{nr}$  of aromatic molecules [119], and substitution of the hydrogen atom in CH-group by either NH<sub>2</sub> or OH-group does not affect  $k_{nr}$  [120]. The two former conditions are only partially satisfied because the introduction of such substitutes as F, NH<sub>2</sub>, etc. into organic molecules may lead (in fact, it does lead) to the redistribution of electron density in the molecule which disturbs the expected dependence of  $k_{nr}(v_{vib}, R)$ .

It has been shown in [120, 121] that NH and OH-groups in free porphyrines and derivative aromatic molecules are more important than CH-groups in terms of contribution to electronic excitation energy (Table 13). Such a strong influence of these substitutes is supposed to result from the interaction between the unshared pair of nitrogen and oxygen atoms and electrons of the ring. This interaction precludes considering NH<sub>2</sub> and OH-groups to be located at a greater distance from the electronic transition site compared with

**Table 13.** Effect of deuteration of NH, OH, and CH-groups in organic molecules on their phosphorescence lifetime in alcoholic solutions at 77 K [120]

Compound	$\tau_{\text{ph}}$ , s (ethanol- $h_6$ )	Compound	$\tau_{\text{ph}}$ , s (ethanol- $d_6$ )
1- $H_2$ -naphthylamine- $h_7$	1.0	1- $D_2$ -naphthylamine- $h_7$	1.4
1- $H_2$ -naphthylamine- $d_7$	2.7	1- $D_2$ -naphthylamine- $d_7$	11.0
2- $H_2$ -naphthylamine- $h_7$	1.2	2- $D_2$ -naphthylamine- $h_7$	1.7
1,5- $H_4$ -naphthalene diamine- $h_6$	0.75	1,5- $D_4$ -naphthalene diamine- $h_6$	1.55
1- $H_3$ -naphthylammonium- $h_7$	1.25	1- $D_3$ -naphthylammonium- $h_7$	1.7
1- $H_3$ -naphthylammonium- $d_7$	2.5	1- $D_3$ -naphthylammonium- $d_7$	10.0
3,6- $H_4$ -diamine-acridine- $h_8$	2.2	3,6- $D_4$ -diamine-acridine- $h_8$	3.0
$H_4$ -tripaflavine- $h_{10}$	2.2	$D_4$ -tripaflavine- $h_{10}$	3.0
$H_4$ -acridine yellow- $h_{11}$	2.1	$D_4$ -acridine yellow- $h_{11}$	2.9
2- $H$ -naphthol- $h_7$	1.3	2- $D$ -naphthol- $h_7$	1.4
2- $H$ -naphthol- $d_7$	4.7	2- $D$ -naphthol- $d_7$	11.0
Ethyl ether	1.9	Ethyl ether	1.9
2-naphthol- $h_{12}$		2-naphthol- $h_{12}$	

Note: Capital  $D$  refers to deuteration of amino and hydroxyl groups, whereas lower-case  $d$  does that for the ring CH-groups.

CH-groups of the same ring. It has been experimentally shown that deuteration of NH-groups of naphthylamine has a greater effect on the  $k_{\text{nr}}$  value of the molecule than deuteration of the same groups in naphthylammonium (see Table 13). This finding indicates that electronic transition in naphthylamine is localised closer to the  $\text{NH}_2$ -group than in naphthylammonium. This inference is supported by the results of spectral studies which have demonstrated that binding of the third hydrogen atom to nitrogen leads to the transformation of the 1-naphthylamine phosphorescence spectrum to a spectrum resembling that of naphthalene. This suggests a higher degree of localisation of electronic transition on the naphthylammonium ring than in naphthylamine.

Thus, the analysis of contributions of individual atomic groups to nonradiative transitions in organic molecules appears to encounter more difficulties than in the case of metal ions since the examination of this process in molecules requires taking into account both localisation of electronic transition and effect of substitute groups on electron density redistribution. Taking into account changes in the localisation of electronic transition during halogenization of organic molecules provides an explanation for the anomalous dependence of  $k_{\text{nr}}$  in naphthalene derivatives on the vibrational frequency of donor-acceptor atomic groups found in a study of halogenated naphthalenes [117]. It is clear that elucidation of nonradiative transition mechanisms in organic molecules by examining  $R$ -dependence of  $k_{\text{nr}}$  is meaningful only when the introduction of substitutes does not alter localisation of electronic excitation. Aliphatic ketones appear to be the most useful objects to study  $k_{\text{nr}}$  dependence on  $R$ . Table 14 shows  $k_{\text{nr}}^{\text{ph}}/k_{\text{r}}^{\text{ph}}$  ratios for a series of ketones as reported by O'Sullivan and Testa [118].

The ketone triplet-singlet  $n - \pi^*$  transition responsible for phosphorescence is known to be located on the  $\text{C}=\text{O}$ -group and is practically unrelated to aliphatic substitutes [122]. The

**Table 14.** Dependence of  $k_{\text{nr}}$  in aliphatic ketones on the distance between the electron transition centre responsible for phosphorescence ( $\text{C}=\text{O}$ -group) and  $\text{C}-\text{H}$ -groups containing localised donor-acceptor oscillations ( $\lambda_{\text{exc}} = 313$  nm,  $\lambda_{\text{obs}} = 450$  nm, EPA, 77 K) (from [118])

Compound	$q_{\text{ph}}$	$k_{\text{nr}}$ , $\text{s}^{-1}$	$k_{\text{r}}$ , $\text{s}^{-1}$
$\text{CH}_3\text{COCH}_3$	0.043	$2.9 \times 10^3$	77
$\text{CD}_3\text{COCD}_3$	0.106	$9.2 \times 10^2$	80
$(\text{CH}_3)_2\text{CHCOCH}(\text{CH}_3)_2$	0.306	$1.8 \times 10^2$	81
$(\text{CH}_3)_3\text{CCOC}(\text{CH}_3)_3$	0.89	16	100

main progression in the phosphorescence spectrum is due to the valent vibration  $\text{C}=\text{O}$ , and there is only a slow decrease of band intensities in the phosphorescence spectrum owing to a greater change of the equilibrium  $\text{C}=\text{O}$  distance in the triplet state as compared with that in the ground state. It follows from Table 14 that the nonradiative transition rate constant rapidly decreases with an increase in the distance between  $\text{C}-\text{H}$ -groups and the  $\text{C}=\text{O}$ -group responsible for phosphorescence.  $\int_{\text{ov}}$  values for the compounds in Table 14 with similar phosphorescence spectra and the vibrational absorption spectrum of the  $\text{C}-\text{H}$ -group do not significantly change. Hence, it is inferred that a 100-fold reduction of the  $k_{\text{nr}}^{\text{ph}}/k_{\text{r}}^{\text{ph}}$  ratio in the above series may be due to the increasing distance between groups with donor-acceptor oscillations and the vibronic transition oscillator in the  $\text{C}=\text{O}$ -group.

To sum up, the  $k_{\text{nr}}(R)$  dependence for organic molecules is as strong as for metal ions in solutions, but its investigation on molecules is much more difficult due to the effect of substitutes on the localisation of electronic excitation and the vibronic spectrum.

An important sequel of the inductive-resonant theory of nonradiative transitions is the proportionality of  $k_{\text{nr}}$  to the overlap integral over luminescence spectra (or phosphorescence spectra of organic molecules) and vibrational absorption spectra of donor-acceptor groups. In organic (in particular, aromatic) molecules donor-acceptor oscillations are largely represented by  $\text{C}-\text{H}(\text{D})$  (less frequently  $\text{N}-\text{H}$  and  $\text{O}-\text{H}$ ) valent oscillations. In an earlier study [13], we compared experimentally found  $k_{\text{nr}}/k_{\text{r}}$  values for the  $T_1 - S_0$ -transition and  $\int_{\text{ov}}$  for some aromatic hydrocarbons, dye, and porphin.

The results of comparing  $k_{\text{nr}}$  and  $\int_{\text{ov}}$  in [13] do not only account for the observed linear  $\Delta E_{\text{el}}$ -dependence of  $\log k_{\text{nr}}$  in certain aromatic molecules but also make it possible to quantitatively explain the two orders of magnitude difference in  $k_{\text{nr}}$  values for dyes and aromatic molecules (e.g., pyrene and acriflavine) having similar  $\Delta E_{\text{el}}$  but a different width of vibronic spectra (i.e. different parameters of heat release) (Table 15).

**Table 15.** Comparison of the rate constant ratio of nonradiative ( $k_{\text{nr}}$ ) to radiative ( $k_{\text{r}}$ ) transitions from the low triplet (phosphorescent) state of aromatic molecules to the ground state and the overlap integrals over phosphorescence spectra and vibrational absorption spectrum of valent oscillations of aromatic  $\text{C}-\text{H}$  groups (alcohol-ether mixture) at 77 K (from [13])

Compound	$\nu_{0,0}^{\text{ph}}$ , $\text{cm}^{-1}$	$k_{\text{nr}}^{\text{ph}}/k_{\text{r}}^{\text{ph}}$	$\int_{\text{ov}}$	$\int_{\text{ov}} / (k_{\text{nr}}^{\text{ph}}/k_{\text{r}}^{\text{ph}})$
Fenanthrene	21700	5	50	10
Naphthalene	21250	24	150	6
Chrysene	20000	10	115	11.5
Pyrene	16930	512	3000	6
Acridine	16900	2.2	21	9
Zn-ethioporphyrine†	14250	12.6	172	13.6

† See Ref. [124].

According to formulas (18), (19), these quantities must be proportional provided the distance between the vibronic oscillator and groups responsible for donor-acceptor oscillations remains unaltered. In order to estimate  $\int_{\text{ov}}$ , we measured phosphorescence spectra of the above compounds and extrapolated the results to the long-wavelength range where their measurement was difficult to perform, using the formula of McCoy and Ross [123]. We also measured vibrational absorption spectra of C–H oscillations for benzene- $h_6$  and benzene- $d_6$  up to 4–6 overtones. Because C–H oscillations are characteristic, these spectra resembled vibrational spectra of other aromatic molecules which allowed for their use in calculating overlap integrals over spectra. The calculation also took into account the number of hydrogen atoms in relation to the number of C, N, and O atoms in the molecule.

These data are tabulated in Table 15. Comparison of columns 3 and 4 reveals a good correlation between  $k_{\text{nr}}/k_{\text{r}}$  and  $\int_{\text{ov}}$  values. Naturally, exact proportionality between  $k_{\text{nr}}/k_{\text{r}}$  and  $\int_{\text{ov}}$  can hardly be expected because the distance between the vibronic oscillator responsible for phosphorescence and the vibrational oscillator of donor-acceptor groups is subject to alteration. Changes in their relative orientation may equally be of some consequence. On the other hand, variation of the overlap integral to  $k_{\text{nr}}/k_{\text{r}}$  ratio for the compounds in question (column 5) is surprisingly small despite a 100-fold change in the absolute constant to constant ratio (column 3). It appears that the efficiency of interaction between the vibronic oscillator of the  $\pi$ -electron system and vibrational C–H oscillators for the compounds included in Table 15 varies insignificantly.

The quantity  $k_{\text{nr}}^{\text{ph}}/k_{\text{r}}^{\text{ph}} = (1 - q_{\text{fl}} - q_{\text{ph}})/q_{\text{ph}}$ , where  $q_{\text{fl}}$  and  $q_{\text{ph}}$  are absolute quantum yields of fluorescence and phosphorescence, respectively. Following [125], it is assumed that deactivation of electronic energy in the above compounds in solid solutions at 77 K proceeds via the triplet state. In other words, nonradiative transitions from the lower-energy singlet (fluorescent) state to the ground state can be disregarded.

The data presented in Table 15 are useful in that they help in clarifying why pyrene and acriflavine having similar energies of the triplet state phosphoresce with so different quantum yields. This case is also illustrated by Fig. 8, which

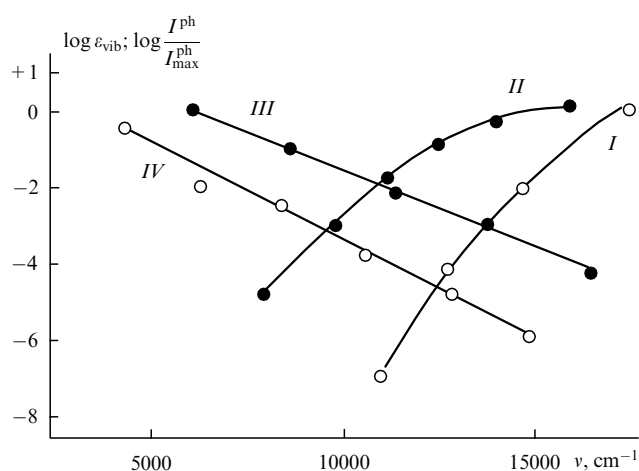


**Figure 8.** Frequency dependences of logarithm of quantum phosphorescence intensity ratios ( $I^{\text{ph}}/I_{\text{max}}^{\text{ph}}$ ) for acriflavine (I) and pyrene (II). Frequency dependences of logarithm of molar absorption coefficient for overtones of valent C–H(D) oscillations in benzene ( $\text{C}_6\text{H}_6$  — III) and ( $\text{C}_6\text{D}_6$  — IV) are also graphed.

shows curves that characterise decreasing intensity of phosphorescence spectra of these two compounds in passing to lower frequencies and a drop of absorption intensity for C–H and C–D valent oscillations of benzene with growing overtone number (increasing frequency). The slower drop of pyrene phosphorescence intensity towards the red edge is responsible for a much larger  $\int_{\text{ov}}$  value, that is, lower phosphorescence efficiency ( $k_{\text{r}}^{\text{ph}}/(k_{\text{r}}^{\text{ph}} + k_{\text{nr}}^{\text{ph}})$ ).

We have already mentioned that there exists proportionality between  $k_{\text{nr}}$  and  $\int_{\text{ov}}$  regardless of the choice of the perturbation operator and the possibility to satisfy conditions for multipolar expansion of electrostatic interaction between electrons and nuclei. This means that the proportionality condition for  $k_{\text{nr}}$  and  $\int_{\text{ov}}$  must be fulfilled for all molecules and actually provides the best way to calculate the Franck–Condon matrix element even though it does not prove the dipole-dipole mechanism of electronic-vibrational interaction.

Experimental evidence of the dipole-dipole mechanism of dissipation of electronic excitation energy in organic molecules has been obtained in Ref. [126], where the direct proportionality between  $k_{\text{nr}}$  and  $k_{\text{r}}$  was observed. The latter was confirmed in a study on deactivation of individual sublevels of triplet molecular states using a few series of related organic compounds [127–129]. The optical-microwave double resonance technique [127–129] was employed to estimate the rates of radiative and nonradiative transitions from individual sublevels of the triplet molecular state at low temperatures ( $< 4$  K). Radiative ( $k_{\text{r}}^x, k_{\text{r}}^y,$  and  $k_{\text{r}}^z$ ) and non-radiative ( $k_{\text{nr}}^x, k_{\text{nr}}^y,$  and  $k_{\text{nr}}^z$ ) transition rate constants for selected compounds are presented in Table 16.

**Table 16.** Comparison of nonradiative transition constants and relative constants for radiative transitions from individual sublevels of the triplet states of organic molecules at  $T < 4.2$  K

Compound (base)	$k_{\text{nr}}^x, \text{s}^{-1}$	$k_{\text{nr}}^y, \text{s}^{-1}$	$k_{\text{nr}}^z, \text{s}^{-1}$	$k_{\text{r}}^x, \text{s}^{-1}$	$k_{\text{r}}^y, \text{s}^{-1}$	$k_{\text{r}}^z, \text{s}^{-1}$	Refs
Quinoxaline ( <i>n</i> -dibromobenzene)	27	9.3	26	1.0	1.0	4.4	[128]
Quinoxaline (durol)	11.1	0.59	0.40	1.0	0.02	0.015	[128]
Benzophenone (monocrystal)	39.1	63.3	633.0	1.0	1.85	16	[127]
Naphthalene- $d_8$ ( <i>n</i> -dibromobenzene)	16.0	15.5	55.0	1.0	1.0	2.2	[128]
1,3-diazanaphthalene (durol)	0.42	1.1	4.0	0.20	1.0	15.6	[129]
1,5-diazanaphthalene (durol)	0.31	0.52	4.4	0.39	1.0	25.5	[129]
1,8-diazanaphthalene (durol)	0.28	0.46	6.3	0.94	1.0	31.0	[129]

Note: Axis  $z$  in aromatic molecules is perpendicular to the plane of the molecule, in benzophenone it runs along the C=O bond.

It follows from Table 16 that experimentally found rate constants for downward nonradiative transitions from individual sublevels of the lower-energy triplet state to the ground state are approximately proportional to the rate constants for radiative transitions from the same levels. We believe it to be further evidence in support of the inductive-resonant theory of nonradiative transitions. Direct proportionality between  $k_{\text{r}}^i$  and  $k_{\text{nr}}^i$  cannot be expected because dipole moments for transitions from individual sublevels of the triplet state differ in direction. Hence, differences between

their interactions with dipole moments of transitions for donor-acceptor oscillations can be affected.

The observed proportionality between  $k_{nr}$  and  $k_r$  sets thinking us about parameters of expansion in multipoles of electronic-vibrational interactions in molecules. Strong dependence of electronic-vibrational interactions with isolated groups of atoms on the localisation site of electronic excitation suggests that the electronic oscillator is smaller in size than the electron cloud of the molecule. The possibility of electronic-vibrational interaction expanding in multipoles remains to be confirmed. The same is true for the identity of proportionalities between  $k_{nr}$  and  $k_r \int_{ov}$  observed in the experiment and characteristic of the dipole-dipole approximation. The absence of direct proportionality between changes of  $k_{nr}$  and  $k_r$  in molecules upon the introduction of a heavy atom reported by certain authors is not in conflict with the inductive-resonant theory because concurrent changes of  $\int_{ov}$  need to be taken into account (see Section 3.2).

To conclude, the inductive-resonant theory of nonradiative transitions is a valuable tool for describing this process in a variety of objects. Trivalent lanthanide ions appear to be the most convenient objects to validate the theory because electronic transitions in these ions are fairly well localised, and the surrounding ligands have but a weak effect on the radiative transition rate constant while nonradiative transition rate constants show strong dependence on the environment of  $\text{Ln}^{3+}$  ions. Comparison of  $k_{nr}$  values obtained in the experiment and calculated using the inductive-resonant theory has demonstrated that the theory is especially useful for the description of the following experimental facts: (1) the effect of substituting D for H in ligands and solvents surrounding  $\text{Ln}^{3+}$  ions; (2)  $k_{nr}$  dependence on the energy gap  $\Delta E$  between the excited and the nearest low-lying electronic level; (3)  $k_{nr}$  dependence on the distance between the ion and the molecular group whose oscillations are responsible for nonradiative transitions; (4) abnormal low  $k_{nr}$  values for electronic transitions that emit in the magnetic dipole-like mode; (5) the theory equally well describes temperature dependence of  $k_{nr}$  for  $\text{Ln}^{3+}$  ions introduced as activators into glasses and crystals, and, finally, (6) more often than not the quantitative calculations of  $k_{nr}$  in the inductive-resonant theory are in good agreement with experimental data.

In a more complicated case of transition metal ions, electronic transition is less strictly localised, and the influence of ligands on the ion's spectroscopic properties is much stronger, as is evidenced by the well-developed vibronic structure. But in this case also, the inductive-resonant theory of nonradiative transitions can be applied to the description of experimentally observed  $k_{nr}$  dependences on different factors, viz.: (1) deuteration effect, (2) temperature, (3) distance between  $k_{nr}$  and donor-acceptor groups of ligands, (4) parallelism of changes in rate constants  $k_{nr}$  and  $k_r$  under certain conditions, and (as follows from the theory) (5) satisfactory agreement between calculated (using the inductive-resonant theory) and observed  $k_{nr}$  for this group of compounds.

The present theory has provided a rational explanation for solvent dependence of  $k_{nr}$  for the singlet oxygen molecule.

Complex organic molecules whose radiative vibronic oscillator is commensurable with the conjugate  $\pi$ -electronic system represent the most complicated objects in the framework of the inductive-resonant theory. However, even in this

case, the theory predicts: (1) proportionality between  $k_{nr}$  for the triplet-singlet transition and the overlap integral over phosphorescence spectra and the vibrational absorption spectrum of C–H-groups in the molecule, and (2) a significant decrease of  $k_{nr}$  with increasing distance to the molecular groups showing highest-frequency oscillations (for localised electronic transitions).

To summarise, the inductive-resonant theory of nonradiative transitions explains all known experimental findings concerning physical mechanisms of nonradiative transitions in lanthanide ions of transition metals and organic molecules in the condensed phase.

## 4. Conclusions

Direct experimental evidence of electronic-vibrational energy transfer has been obtained by different authors [36, 130] and is no longer a matter of controversy.

Interpretation of nonradiative transitions as a form of energy transfer is by no means new [131–134], but it has never focused on the mechanisms underlying this process. The inductive-resonant mechanism of nonradiative transitions suggested in 1971 [8, 9] was immediately supported by Th Forster, the author of the theory of inductive-resonant energy transfer between electronic levels [135]. Later, its description used to be included in monographs and reviews [2, 3]. Unfortunately, most of them discuss applicability of this mechanism only to multiphonon transitions in weakly coupled systems with strong anharmonism of atomic oscillations. The present review demonstrates that the sphere of applicability of the inductive-resonant mechanism of nonradiative transitions is much broader. Also, it shows that this mechanism is not at variance with the description of nonradiative transitions through the non-adiabaticity operator; it rather ensues from such a description.

Comparison of theoretical and experimental findings indicates that the inductive-resonant mechanism of nonradiative transitions may be applied to the description of one- and multiphonon transitions in systems with large and small anharmonism of base oscillations. It is equally applicable to the description of the probability of transitions in systems with weak, moderate, and strong strengths of vibronic coupling. According to this approach, a change in the coupling strength causes redistribution of a fraction of energy dissipated on donor-acceptor and acceptor oscillations rather than alteration of the nonradiative transition mechanism. The only limitation on the applicability of the Forster–Galanin–Dexter formulas to the description of nonradiative transitions is imposed by the non-fulfillment of the condition of multipolar expansion of electrostatic interaction between the vibronic transition oscillator and nuclear vibrational oscillators. But even in this case, the calculation of the overlap integral over the ion's or molecule's luminescence spectrum and the vibrational absorption spectrum of atomic groups near the site of electronic excitation localisation makes the best way to calculate the Franck–Condon factor of nonradiative transitions. Because it simultaneously takes into account the shift and the distortion of the potential surfaces for interacting states, anharmonism of all oscillations involved in energy dissipation, and allows for partial separation of oscillations. The calculation of  $\int_{ov}$  is considered to be the best method for the description of  $k_{nr}(T, \Delta E_{el}, \nu_{vib})$  dependence. Analysis of this dependence makes it possible to differentiate, based on experimental data, between the

physical and chemical mechanisms of nonradiative transitions.

We hope that the present review will promote more extensive use of the inductive-resonant theory in calculating  $k_{nr}$  for ions of transition metals and simple molecules in solutions, glasses, and molecular crystals, and also in describing nonradiative transition mechanisms for metal ions in low-frequency bases and complex polyatomic molecules. It may be expected that experimental data on the effect of substitutive groups on  $k_{nr}$  will be useful in pinpointing the site of electronic excitation localisation in these molecules.

We wish to acknowledge the support of the Russian Fund for Basic Research (Project No. 94-02-06192).

## References

- Landau L D, Lifshitz E M *Quantum Mechanics* 3rd edition (Oxford: Pergamon, 1977)
- Englman R *Non-Radiative Decay of Ions and Molecules in Solids* (Amsterdam: North Holland, 1979) p. 336
- Medvedev E S, Oshero V I *Radiationless Transitions in Polyatomic Molecules* (Berlin: Springer-Verlag, 1995)
- Ermolaev V L, Bodunov E N, Svshnikova E B, Shakhverdov T A *Bezyzluchatel'nyi Perenos Énergii Électronnogo Vozbuzhdeniya* (Nonradiative Transfer of Electronic Excitation Energy) (Moscow: Nauka, 1977) Ch. 8
- Kaminskiĭ A A et al. *Fizika i Spektroskopiya Lazernykh Kristallov* (Physics and Spectroscopy of Laser Crystals) (Moscow: Nauka, 1986) Part 3
- Calvert J G, Pitts J N (Jr) *Photochemistry* (New York, London: J Wiley and Sons, 1966)
- Kaminskiĭ A A, Antipenko B M *Mnogourovnevye Funktsional'nye Skhemy Kristallicheskiĭh Lazero*v (Multilayer Functional Schemes of Crystal Lasers) (Moscow: Nauka, 1989) p. 270
- Svshnikova E B, Ermolaev V L *Izv. Akad. Nauk SSSR Ser. Fiz.* **35** 1481 (1971)
- Ermolaev V L, Svshnikova E B *Opt. Spektrosk.* **30** 208 (1971)
- Forster Th *Fluoreszenz Organischer Verbindungen* (Göttingen: Hubert und Co, 1951) p. 309
- Li M et al. *J. Chem. Phys.* **97** 4421 (1993)
- Nitzan A, Jortner J, Rentzepis P M *Proc. R. Soc. (London)* **A 327** 367 (1972)
- Ermolaev V L, Svshnikova E B *Chem. Phys. Lett.* **23** 349 (1973)
- Bodunov E N *Opt. Spektrosk.* **40** 942 (1976) [*Opt. Spectrosc.* **40** 537 (1976)]
- Agranovich V M, Galanin M D *Perenos Énergii Vozbuzhdeniya v Kondensirovannykh Sredakh* (Energy Excitation Transfer in Condensed Media) (Moscow: Nauka, 1978) p. 383
- Forster Th *Ann. Phys.* **2** (1, 2) 55 (1948)
- Dexter D L *J. Chem. Phys.* **21** 836 (1953)
- Sverdlov L M, Kovner M A, Kraĭnov B P *Kolebatel'nye Spektry Mnogoatomnykh Molekul* (Vibrational Spectra of Polyatomic Molecules) (Moscow: Nauka, 1980) p. 559 [Translated into English (New York: Wiley, 1974)]
- Dean P, in *Vychislitel'nye Metody v Teorii Tverdogo Tela* (Computer Techniques in the Theory of Solids) (Moscow: Mir, 1975) p. 209; Dean P *Rev. Mod. Phys.* **44** 127 (1972)
- Stavola M, Dexter D L *Phys. Rev. B: Cond. Matter* **20** 1867 (1979)
- Huang K, Rhys A *Proc. R. Soc. A* **204** 406 (1950)
- Lax M *J. Chem. Phys.* **20** 1752 (1952)
- Kovarskiĭ V A *Kinetika Bezyzluchatel'nykh Protse*ssov (Kinetics of Nonradiative Processes) (Kishinev: AN Mold. SSR, 1968)
- Ridley B K *J. Phys. C.: Sol. St. Phys.* **11** 2323 (1978)
- Helmis G *Ann. Phys. (Leipzig)* **19** 41 (1957)
- Pässler R *Czech. J. Phys. B* **24** 322 (1974)
- Huang K *Scientia Sinica* **24** 27 (1981)
- Kovarskiĭ V A, Perel'man N F, Averbukh I Sh *Mnogokvantovye Protse*ssy (Multiphoton Transitions) (Moscow: Ergoatomizdat, 1985) p. 161
- Bodunov E N, Svshnikova E B *Opt. Spektrosk.* **36** 340 (1974) [*Opt. Spectrosc.* **36** 196 (1974)]
- Pukhov K K *Fiz. Tverd. Tela (Leningrad)* **31** 144 (1989)
- Pukhov K K, Sakun V P *Phys. Status Solidi B* **95** 391 (1979)
- Balagura O V, Ivanov A I *Opt. Spektrosk.* **62** 1043 (1987) [*Opt. Spectrosc.* **62** 616 (1987)]
- Perlin Yu E, Kaminskiĭ A A, Alifanov O V *Fiz. Tverd. Tela (Leningrad)* **29** 3296 (1987) [*Sov. Phys. Solid State* **29** 1890 (1987)]
- Abakumov V N et al. *Zh. Eksp. Teor. Fiz.* **89** 1472 (1985) [*Sov. Phys. JETP* **62** 853 (1985)]
- Jorgensen C K, Judd B R *Mol. Phys.* **8** 281 (1964)
- Gellermann W, Luty F *Opt. Commun.* **72** 214 (1989)
- Kropp J L, Windsor M W *J. Chem. Phys.* **39** 2769 (1963); **42** 1599 (1965)
- Kazanskaya N A, Svshnikova E B *Opt. Spektrosk.* **28** 699 (1970) [*Opt. Spectrosc.* **28** 376 (1970)]
- Gallagher P K *J. Chem. Phys.* **43** 1742 (1965)
- Heller A J. *Am. Chem. Soc.* **89** 167 (1967)
- Ermolaev V L, Svshnikova E B *Usp. Khim.* **63** 962 (1994)
- Ermolaev V L, Svshnikova E B, Tachin V S *Opt. Spektrosk.* **41** 341 (1976)
- Dieke G H, Crosswhite H M *Appl. Opt.* **2** 675 (1963)
- Galanin M D, Frank I M *Zh. Eksp. Teor. Fiz.* **21** 114 (1951)
- Svshnikova E B, Serov A P, Kondakova V P *Opt. Spektrosk.* **39** 285 (1975)
- Svshnikova E B, Naumov S P, Shakhverdov T A *Opt. Spektrosk.* **42** 920 (1977) [*Opt. Spectrosc.* **42** 529 (1977)]
- Bunzli J-C G, Choppin G R (Eds) *Lanthanide Probes in Life. Chemical and Earth Sciences. Theory and Practice* (Amsterdam: Elsevier, 1989)
- Balzani V, Sabbatini N *Chem. Rev.* **86** 331 (1986)
- Svshnikova E B *Induktivno-Resonansnyi Mekhanizm Bezyzluchatel'nykh Perekhodov Mezhdu Élektronnymi Urovniami* Dis. doct. (Inductive-Resonant Mechanism of Nonradiative Transitions Between Electronic Levels. Doctoral dissertation) (Leningrad: S I Vavilov Optical Institute, 1984)
- Svshnikova E B, Naumov S P *Opt. Spektrosk.* **44** 127 (1978)
- Svshnikova E B, Timofeev N T *Opt. Spektrosk.* **48** 503 (1980) [*Opt. Spectrosc.* **48** 276 (1980)]
- Ermolaev V L, Svshnikova E B *J. Lumin.* **20** 387 (1979)
- Basiev T T et al. *Trudy IOFAN* **46** 3 (1994)
- Timofeev N T, Svshnikova E B *Opt. Spektrosk.* **51** 833 (1981)
- Hehlen M P, Reisen H, Gudel H U *Inorg. Chem.* **30** 2273 (1991)
- Van Dijk J M F *J. Lumin.* **24/25** 705 (1981)
- Cossy C, Merbach A E *Pure Appl. Chem.* **60** 1785 (1988)
- Perelygin I S, Klimchuk M A *Zh. Prikl. Spektrosk.* **20** 907 (1974)
- Perlin Yu E, Alifanov O V *Izv. Akad. Nauk SSSR Ser. Fiz.* **54** 406 (1990)
- Svshnikova E B, Neporent I B *Izv. Akad. Nauk SSSR Ser. Fiz.* **37** 378 (1973)
- May P S, Richardson F S *Chem. Phys. Lett.* **179** 277 (1991)
- Blasse G, Dirksen G J *J. Solid State Chem.* **96** 258 (1992)
- Svshnikova E B, Timofeev N T, Zolotarev V M *Izv. Akad. Nauk SSSR Ser. Fiz.* **44** 722 (1980)
- Svshnikova E B et al. *Opt. Spektrosk.* **54** 259 (1983) [*Opt. Spectrosc.* **54** 153 (1983)]
- Gapontsev V P, Sirtlanov M R, Yen W J *Lumin.* **31/32** 201 (1984)
- Gapontsev V P, Sirtlanov M R, Isynee V A *Proc. Intern. Conf. in Lasers-81* (STS-press, 1982) p. 763
- Avanesov A G et al. *Zh. Eksp. Teor. Fiz.* **77** 1771 (1979) [*Sov. Phys. JETP* **50** 886 (1979)]
- Gapontsev V P *Pis'ma Zh. Eksp. Teor. Fiz.* **29** 234 (1979) [*JETP Lett.* **29** 210 (1979)]
- Svshnikova E B, Stroganov A A, Urusovskaya L N *Opt. Spektrosk.* **63** 1047 (1987)
- Svshnikova E B, Stroganov A A, Timofeev N T *Opt. Spektrosk.* **64** 73 (1988)
- Bottger H *Principles of the Theory of Lattice Dynamics* (Berlin: Acad. Verlag, 1983)
- Mills D L, Duthler C J, Sparks M, in *Dynamical Properties of Solids. Disorder Solids Optical Properties* Vol. 4 (New York, 1980) p. 379
- Riseberg L A, Moos H W *Phys. Rev.* **174** 429 (1968)
- Miller M P, Wright J C *J. Chem. Phys.* **71** 324 (1979)
- Layne C B, Lowdermilk W H, Weber M J *Phys. Rev. B* **16** 10 (1977)

76. Riseberg L A, Weber M J, in *Progress in Optics* Vol. 14 (Amsterdam: Elsevier, 1976) p. 89
77. Reed E D, Moos H W *Phys. Rev. B* **8** 980 (1973)
78. Lipson H G et al. *Phys. Rev. B* **13** 2614 (1976)
79. Svshnikova E B, Stroganov A A *Izv. Akad. Nauk SSSR Ser. Fiz.* **52** 725 (1988)
80. Henderson B, Imbush G F *Optical Spectroscopy of Inorganic Solids* (Oxford: Clarendon Press, 1989)
81. Crosby G A *Account Chem. Res.* **8** 231 (1975)
82. Pennzkofer A, in *Progress in Quantum Electronics* **12** 291 (1988)
83. Svshnikova E B, Timofeev N T *Zh. Prikl. Spektrosk.* **55** 832 (1991)
84. Sviridov D T, Sviridova R K, Smirnov Yu F *Opticheskie Spektiry Ionov Perekhodnykh Metallov v Kristallakh* (Optical Spectra of Transition Metal Ions in Crystals) (Moscow: Nauka, 1976) p. 267
85. Svshnikova E B, Neporent I B *Opt. Spektrosk.* **35** 486 (1973)
86. Neporent I B, Svshnikova E B, Serov A P *Izv. Akad. Nauk SSSR Ser. Fiz.* **39** 1959 (1975) [*Bull. Acad. Sci. USSR* **39** 155 (1975)]
87. Svshnikova E B *Izv. Akad. Nauk SSSR Ser. Fiz.* **39** 1801 (1975)
88. Svshnikova E B, Naumov S P *Opt. Spektrosk.* **45** 505 (1978) [*Opt. Spectrosc.* **45** 283 (1978)]
89. Jia W, Strauss E, Yen W M *J. Lumin.* **45** 451 (1990)
90. Svshnikova E B, Stroganov A A *Opt. Spektrosk.* **60** 521 (1986) [*Opt. Spectrosc.* **60** 320 (1986)]
91. Sell D D et al. *J. Appl. Phys.* **37** 1229 (1966)
92. Ermolaev V L, Svshnikova E B *Opt. Spektrosk.* **68** 780 (1990)
93. Svshnikova E B, Naumov S P *Opt. Spektrosk.* **47** 502 (1979) [*Opt. Spectrosc.* **47** 279 (1979)]
94. Naumov S P, Svshnikova E B *Opt. Spektrosk.* **45** 903 (1978) [*Opt. Spectrosc.* **45** 761 (1978)]
95. Stone M L, Crosby G A *Chem. Phys. Lett.* **79** 169 (1981)
96. Myrick M L, Blakley R L, De Armond M K *Chem. Phys. Lett.* **157** 73 (1989)
97. Reber C, Gudel H U *J. Lumin.* **42** 1 (1988)
98. Svshnikova E B, Teneshev L N *Opt. Spektrosk.* **70** 568 (1991)
99. Suzuki Y et al. *Phys. Rev. B* **35** 4472 (1987)
100. Gapontsev V P et al., in *Bezyzluchatel'naya Relaksatsiya Trekhvalentnogo Khroma v Stekloobraznykh Sredakh* (Nonradiative Relaxation of Trivalent Chromium in Glassy Media) Vol. 12 (Preprint of Instituta radiotekhniki i elektroniki AN SSSR, 1985)
101. Svshnikova E B et al. *Opt. Spektrosk.* **68** 785 (1990)
102. Weber M J, Brawer S A, DeGroot A J *Phys. Rev. B* **23** 11 (1981)
103. Artsybysheva I B et al. *Opt. Spektrosk.* **62** 934 (1987) [*Opt. Spectrosc.* **62** 556 (1987)]
104. Hurst J R, Schuster G B *J. Am. Chem. Soc.* **105** 5756 (1983)
105. Ogilby P K, Foote C S *J. Am. Chem. Soc.* **105** 3423 (1983)
106. Rodgers M A J. *Photochem.* **25** 127 (1984)
107. Alshari E, Schmidt R *Chem. Phys. Lett.* **128** 184 (1991)
108. Egorov S Y et al. *Chem. Phys. Lett.* **163** 421 (1989)
109. Schmidt R *J. Am. Chem. Soc.* **111** 6983 (1989)
110. Merkel P B, Kearns D R *J. Am. Chem. Soc.* **94** 7244 (1972)
111. Svshnikova E B, Minaev B F *Opt. Spektrosk.* **54** 542 (1983) [*Opt. Spectrosc.* **54** 320 (1983)]
112. Salokhiddinov K I, Buteva I M, Dzhagarov B M *Opt. Spektrosk.* **47** 881 (1979) [*Opt. Spectrosc.* **47** 487 (1979)]
113. Mortensen O S, Siebrand W, Tarr A W *Chem. Phys.* **125** 231 (1988)
114. Henry B R, Siebrand W, in *Organic Molecular Photophysics* Vol. 1 (New York, London: Academic, 1973) p. 157
115. Hutchison C A, Mangum B W *J. Chem. Phys.* **32** (4) 1261 (1960)
116. Hammond G S, in *Advances in Photochemistry* Vol. 7 (New York, London, 1969) p. 373
117. Ermolaev V L, Svshnikova E B *Opt. Spektrosk.* **21** 134 (1966) [*Opt. Spectrosc.* **21** (1) 78 (1966)]
118. O'Sullivan M, Testa A C *J. Am. Chem. Soc.* **92** 258 (1970)
119. Henry B R, Charlton J L *J. Am. Chem. Soc.* **95** 2782 (1973)
120. Svshnikova E B, Kondakova V P *Opt. Spektrosk.* **50** 870 (1981) [*Opt. Spectrosc.* **50** 477 (1981)]
121. Solov'ev K N et al. *Opt. Spektrosk.* **41** 964 (1976) [*Opt. Spectrosc.* **41** 569 (1976)]
122. Kasha M *Discuss. Faraday Soc.* **9** 14 (1950); *Radiat. Res. Suppl.* **2** 243 (1960)
123. McCoy E F, Ross I G *Australian J. Chem.* **15** 573 (1962)
124. Gradyushko A T, Tsvirko M P *Opt. Spektrosk.* **31** 548 (1971) [*Opt. Spectrosc.* **31** 291 (1971)]
125. Ermolaev V L, Svshnikova E B *Acta Phys. Pol.* **15** (11) 771 (1968)
126. Zander M, Rutgerswerke A G *Z. Naturforsch.* **43** 393 (1988)
127. Winscom C J, Maki A H *Chem. Phys. Lett.* **12** 264 (1971)
128. Cheng T H, Hirota N, Mao S W *Chem. Phys. Lett.* **15** 274 (1972)
129. Gromer J, Sixl H, Wolf H C *Chem. Phys. Lett.* **12** 574 (1972)
130. Hunter T F, Kristjansson K S *Chem. Phys. Lett.* **75** 456 (1980)
131. Heber J *Phys. Kondens. Mater.* **6** 381 (1967)
132. Ballard R E *Spectrochim. Acta* **24 A** 65 (1968)
133. Terpilovskii L I *Opt. Spektrosk.* **24** 596 (1968)
134. Franck J, Sponer H *J. Chem. Phys.* **25** (1) 172 (1956)
135. Forster Th *Chem. Phys. Lett.* **12** 422 (1971)